



UNIVERSITY  
OF  
JOHANNESBURG

## **Development and Characterisation of a propriety polymer matrix for enhanced optical properties**

A dissertation submitted to the Faculty of Health Sciences,  
University of Johannesburg, in fulfilment of the requirements for the  
degree of

Master of Technology: Biomedical Technology

by

Fezile Khumalo

(Student number 920406395)

Supervisor \_\_\_\_\_

Prof. H. Abrahamse

\_\_\_\_\_

Date

Co-Supervisor \_\_\_\_\_

Dr. R. Sparrow

\_\_\_\_\_

Date

Co-Supervisor \_\_\_\_\_

Dr. J. Jordaan

\_\_\_\_\_

Date

Pretoria, 2010

## DECLARATION

I declare that this dissertation is my own, unaided work. It is being submitted for the Degree of Master of Technology at the University of Johannesburg. It has not been submitted before for any degree or examination in any other University.

---

F. B. Khumalo

\_\_\_\_\_ Day of \_\_\_\_\_ 2010





## AFFIDAVIT: MASTER'S AND DOCTORAL STUDENTS TO WHOM IT MAY CONCERN

This serves to confirm that I \_\_\_\_\_ Fezile Khumalo \_\_\_\_\_  
(Full Name(s) and Surname)

ID Number \_\_\_\_\_ 8604140409088 \_\_\_\_\_

Student number \_\_\_\_\_ 920406395 \_\_\_\_\_ enrolled for the

Qualification \_\_\_\_\_ M Tech Biomedical Technology \_\_\_\_\_

Faculty \_\_\_\_\_ Health Sciences \_\_\_\_\_

Herewith declare that my academic work is in line with the Plagiarism Policy of the University of Johannesburg which I am familiar with.

I further declare that the work presented in the \_\_\_\_\_  
(minor dissertation/dissertation/thesis) is authentic and original unless clearly indicated otherwise and in such instances full reference to the source is acknowledged and I do not pretend to receive any credit for such acknowledged quotations, and that there is no copyright infringement in my work. I declare that no unethical research practices were used or material gained through dishonesty. I understand that plagiarism is a serious offence and that should I contravene the Plagiarism Policy notwithstanding signing this affidavit, I may be found guilty of a serious criminal offence (perjury) that would amongst other consequences compel the UJ to inform all other tertiary institutions of the offence and to issue a corresponding certificate of reprehensible academic conduct to whomever request such a certificate from the institution.

Signed at \_\_\_\_\_ Pretoria \_\_\_\_\_ on this \_\_\_\_\_ 17 \_\_\_\_\_ day of \_\_\_\_\_ May \_\_\_\_\_ 20\_10\_.

Signature \_\_\_\_\_ Print name \_\_\_\_\_

### STAMP COMMISSIONER OF OATHS

#### Affidavit certified by a Commissioner of Oaths

This affidavit conforms with the requirements of the JUSTICES OF THE PEASE AND COMMISSIONERS OF OATHS ACT 16 OF 1963 and the applicable Regulations published in the GG GNR 1258 of 21 July 1972; GN 903 of 10 July 1998; GN 109 of 2 February 2001 as amended.

## ABSTRACT

Well defined micron sized particles are used in applications ranging from immunoassay detection agents to enzyme immobilisation supports. The market for microparticles is constantly changing and expanding and developments in particle technologies need to meet these advancements as well as act as enabling systems to realise new applications. Chromophoric and/or fluorescent particles have a broad range of applications. Of particular interest is their application as detection agents for rapid diagnostic applications. Developments in improving particles as detection agents concentrate on improving their visual (colour intensity), optical properties, particle size, and biological binding capacity. This study aimed to evaluate the application of ReSyn™ (WO2009057049) particles as detection agents.

The study investigated three parameters that are important for the application of microparticles. These are particle size, particle size distribution and optical properties. Using an emulsion based technique particle sizes of 6, 13 and 20µm were prepared. These particles were further bound to different dyes to improve their visual properties. The particles demonstrated a higher binding capacity when compared to particle technologies currently available on the market. These particles bound up to 54% dye of the final dry weight. Dyes with distinct spectral wavelengths were used to illustrate the particle technology's potential to be applied in bead based multiplex assays.

The capacity for ReSyn™ for possible application as a detection agent in diagnostics and multiplex assays has been demonstrated with the high dye binding capacity and the ability to control particle size. These properties confer good visibility with potential to improve particle detectability; the ability to control particle sizes offers the possibility of realising more applications. However, further improvements are required to realise these applications, including controlling the emulsion parameters for producing more uniform particles. These particles will be further developed for application as detection agents.

## Acknowledgements

---

I would like to extend my sincerest appreciation to the following people whose support both professionally and personally has been invaluable.

Dr Raymond Sparrow (Co-Supervisor) - a special thank you for the support and guidance in my academic career. Your experience and wisdom has been a gift to me. Thank you for the opportunity and recognising the potential in me.

Dr Justin Jordaan (Co-Supervisor) - thank you for the amount of time and patience you have willingly given. Your contribution towards my studies has allowed me to achieve my goals and set my sites on bigger challenges.

Prof H. Abrahamse (Academic Supervisor) - for the endless opportunities and support you have provided over the years. Your direction has allowed me to dream big.

University of Johannesburg and CSIR Biosciences- for the financial support during my studies

To my mother for the unyielding support and faith in my abilities, this would have been harder without you in my corner, Ngiyabonga maThwala.

SisNana, Musa, Phathi and Andi, your love, support and visits kept me motivated to finish.

My friends and family for putting up with me and still believing my madness isn't contagious

Students of Biosciences, Synthetic Biology group those that have come and gone and those that are still around especially, Nanky, Busi, Pila, Olona, Pauline and Mapaledi. I could not have found a greater group of people to enjoy this journey with. You have been friends and motivators during the good and the "could be better" moments of my life.

MSM, MMM team - whom I started with on this path. It was a pleasure working and discovering microfluidics with you.

Tiyani (Biosciences, Aptemer group) - for allowing me to use the microscope

Dr Ben Loos and Dr Rob Smith (University of Stellenbosch) - for their help with understanding flow cytometry and hosting me during my visit there.

Dr Kobie Smit- for being there when I needed to vent when things got heated.

“Tell me and I'll forget; show me and I may remember; involve me and I'll understand” - Chinese proverb



## TABLE OF CONTENTS

|                                   |     |
|-----------------------------------|-----|
| <b>DECLARATION</b>                | i   |
| <b>AFFIDAVIT</b>                  | ii  |
| <b>ABSTRACT</b>                   | iii |
| <b>ACKNOWLEDGEMENTS</b>           | ivi |
| <b>TABLE OF CONTENTS</b>          | vi  |
| <b>LIST OF FIGURES AND TABLES</b> | xi  |
| <b>LIST OF ABBREVIATIONS</b>      | xvi |
| <b>CHAPTER 1</b>                  | 1   |
| <b>INTRODUCTION</b>               | 1   |
| <b>1.1 BACKGROUND</b>             | 2   |
| <b>1.2 PROBLEM STATEMENT</b>      | 4   |
| <b>1.3 AIM</b>                    | 4   |
| <b>CHAPTER 2</b>                  | 5   |
| <b>LITERATURE REVIEW</b>          | 5   |

|                                                               |    |
|---------------------------------------------------------------|----|
| <b>2.1 Applications of microparticles</b>                     | 6  |
| <b>2.1.1 Diagnostic detection agents</b>                      | 6  |
| <b>2.1.2 Research detection agents</b>                        | 11 |
| <b>2.1.3 Detection agents for flow cytometry</b>              | 13 |
| <b>2.1.4 Enzyme immobilisation</b>                            | 17 |
| <b>2.1.5 Microfluidics</b>                                    | 17 |
| <b>2.2 Factors influencing applications of microparticles</b> | 19 |
| <b>2.3 ReSyn™ technology description</b>                      | 20 |
| <b>2.4 Properties of microparticles</b>                       | 21 |
| <b>2.4.1 Microparticle size distribution</b>                  | 21 |
| <i>2.4.1.1 Surfactants</i>                                    | 22 |
| <i>2.4.1.2 Energy impact on emulsification</i>                | 24 |
| <b>2.4.2 Optical properties of microparticles</b>             | 24 |
| <b>2.5 Objectives</b>                                         | 25 |
| <b>CHAPTER 3</b>                                              | 26 |
| <b>METHODOLOGY</b>                                            | 26 |



|                                                                                |    |
|--------------------------------------------------------------------------------|----|
| <b>3.1 Particle preparation</b>                                                | 27 |
| <b>3.2 Evaluation of emulsion parameters for particle size differentiation</b> | 29 |
| <b>3.3 Particle Analysis</b>                                                   | 29 |
| <b>3.3.1 Particle Yield</b>                                                    | 29 |
| <b>3.3.2 Particle size distribution</b>                                        | 29 |
| <b>3.3.3 Flow Cytometry</b>                                                    | 30 |
| <b>3.3.4 Microscopic analysis</b>                                              | 30 |
| <b>3.3.5 Particle density determination</b>                                    | 30 |
| <b>3.4 Particle Dyeing</b>                                                     | 31 |
| <b>3.4.1 Dying of ReSyn™ particles</b>                                         | 31 |
| <b>3.4.2 Evaluation of dye-particle interactions</b>                           | 31 |
| <i>3.4.2.1 Optimum wavelength determination</i>                                | 32 |
| <i>3.4.2.2 Dye binding capacity quantification</i>                             | 32 |
| <b>CHAPTER 4</b>                                                               | 33 |
| <b>RESULTS AND DISCUSSIONS</b>                                                 | 33 |

|                                                                                        |           |
|----------------------------------------------------------------------------------------|-----------|
| <b>4.1 Particle Preparation</b>                                                        | <b>34</b> |
| <b>4.2 Emulsion energy calculations</b>                                                | <b>35</b> |
| <b>4.3 Dry weight determination</b>                                                    | <b>37</b> |
| <b>4.4 Particle size distribution analysis</b>                                         | <b>38</b> |
| <b>4.5 Flow cytometric analysis</b>                                                    | <b>40</b> |
| <b>4.6 Morphological characterisation and analysis using<br/>microscopy</b>            | <b>42</b> |
| <b>4.7 Particle density determination</b>                                              | <b>43</b> |
| <b>4.8 Dye binding capacity of the dyes</b>                                            | <b>44</b> |
| <b>4.8.1 The absorbance spectra of RBBR, Congo Red and Brilliant<br/>    Yellow</b>    | <b>44</b> |
| <b>4.8.2 Percentage dye binding capacities of the different particle<br/>    sizes</b> | <b>46</b> |
| <b>4.8.3 Microscopic analysis of coloured particles</b>                                | <b>50</b> |
| <b>4.9 Technology comparison</b>                                                       | <b>51</b> |
| <b>CHAPTER 5</b>                                                                       | <b>55</b> |
| <b>CONCLUSIONS</b>                                                                     | <b>55</b> |

|                   |    |
|-------------------|----|
| <b>REFERENCES</b> | 58 |
|-------------------|----|

|                   |    |
|-------------------|----|
| <b>APPENDICES</b> | 72 |
|-------------------|----|

|            |    |
|------------|----|
| Appendix 1 | 72 |
|------------|----|

|            |    |
|------------|----|
| Appendix 2 | 74 |
|------------|----|

|            |    |
|------------|----|
| Appendix 3 | 75 |
|------------|----|

|            |    |
|------------|----|
| Appendix 4 | 76 |
|------------|----|



**LIST OF FIGURES AND TABLES**

| <b>Figure</b>    | <b>Title</b>                                                                                                                                                                                                                                                                                                                                                                                                                                                                                                                                                                                                                | <b>Pg<br/>no.</b> |
|------------------|-----------------------------------------------------------------------------------------------------------------------------------------------------------------------------------------------------------------------------------------------------------------------------------------------------------------------------------------------------------------------------------------------------------------------------------------------------------------------------------------------------------------------------------------------------------------------------------------------------------------------------|-------------------|
| <b>Figure 1:</b> | <b>Representation demonstrating the principle of lateral flow assay technology. (a) Free Ab used as a control and an antibody specific to the antigen of interest is bound to coloured microparticles used as detection agents. (b) Conjugation of antigen with antibody bound microparticles followed by migration to the test line. (c) Reaction of Ab-Ag conjugates with another Ab at the test line as well as binding of free Ab in the control line (reproduced from Bell <i>et al.</i>, 2006).</b>                                                                                                                   | <b>6</b>          |
| <b>Figure 2:</b> | <b>A typical rapid diagnostic test and the interpretation of the results. (a) Test strip before the application of sample, no distinct colour is visible. (b) Positive result, change in colour in the test and control region. Distinct and consistent colour bands appear on the control and test regions. Colour intensity of the bands may vary according to concentration of Ag of interest. (c) Negative result only one line appears in the control region. (d) Invalid test, no line appears in the control or test region. (e) Invalid test when the test line changes colour while the control line does not.</b> | <b>7</b>          |
| <b>Figure 3:</b> | <b>Improving signal amplification for lateral flow diagnostic using dual AuNP system. The 1<sup>st</sup> AuNP is conjugated with the Ab specific for the analyte of interest and blocked with BSA. The 2<sup>nd</sup> AuNP is conjugated with anti-BSA Ab to bind specifically with the 1<sup>st</sup> AuNP conjugate to amplify the signal generated from the 1<sup>st</sup> AuNP.</b>                                                                                                                                                                                                                                     | <b>9</b>          |

|                  |                                                                                                                                                                                                                                                                                                                                                                                                                                                                                                                                                                         |           |
|------------------|-------------------------------------------------------------------------------------------------------------------------------------------------------------------------------------------------------------------------------------------------------------------------------------------------------------------------------------------------------------------------------------------------------------------------------------------------------------------------------------------------------------------------------------------------------------------------|-----------|
| <b>Figure 4:</b> | <b>Scheme indicating application of AuNP as contrast agents (not drawn to scale, AuNP (~10-40 nm), DNA (~60 kDa) and or proteins (~20-30 kDa). The AuNP allow the labelling of the cell or parts of the cell for visualisation. The insert shows a AuNP that has been functionalised with an Ab adsorbed to its surface and used as a contrast agent and targeted delivery and or attachment of biomolecules (reproduced from Sperling <i>et al.</i>, 2008).</b>                                                                                                        | <b>11</b> |
| <b>Figure 5:</b> | <b>TEM images of AuNP of various sizes trapped inside vesicles of HeLa cells. Images B- F are AuNP with sizes 14, 30, 50, 74 and 100 nm respectively, gold particles are used as contrast agents (reproduced from Chithrani <i>et al.</i>, 2006).</b>                                                                                                                                                                                                                                                                                                                   | <b>12</b> |
| <b>Figure 6:</b> | <b>Diagram showing how the bead-based flow cytometric technology operates. When the sample in suspension buffer is run through the cytometer, it is hydrodynamically focused, using sheath fluid, through a small nozzle. The tiny 'stream' of fluid takes the particles past the laser light one bead at a time. There are a number of detectors to detect the light scattered from the particles as they go through the beam. The insert shows beads of the same size with different intensities of the same fluorophore and functionalised for specific binding.</b> | <b>14</b> |
| <b>Figure 7:</b> | <b>Coded beads used in multiplex assays. The beads are coded with unique tags, chromophores or fluorophores for easy identification upon detection (reproduced from Birtwell <i>et al.</i>, 2010).</b>                                                                                                                                                                                                                                                                                                                                                                  | <b>15</b> |

|                   |                                                                                                                                                                                                                                                                                                                                                                         |    |
|-------------------|-------------------------------------------------------------------------------------------------------------------------------------------------------------------------------------------------------------------------------------------------------------------------------------------------------------------------------------------------------------------------|----|
| <i>Figure 8:</i>  | Micro channels (100 $\mu\text{m}$ ) used in the development of miniaturised immunoassays. (a) Functionalised microparticles are conjugated to specific Ab and attached to the microchannel surface. The particles provide increased surface area for improved sensitivity. (b) Alternative limited sensitivity; Ab are attached directly onto the microchannel surface. | 17 |
| <i>Figure 9:</i>  | Illustration of a ReSyn™ particle. The particles formed are spherical and contain a high density of functional groups.                                                                                                                                                                                                                                                  | 20 |
| <i>Figure 10:</i> | Alignment of surfactant molecules during emulsification to form stable emulsion droplets. The hydrophobic tails orientate themselves and give stability to the formed emulsion droplets.                                                                                                                                                                                | 23 |
| <i>Figure 11:</i> | The particle preparation process as described in 2.1                                                                                                                                                                                                                                                                                                                    | 28 |
| <i>Figure 12:</i> | Image of the formed particles prior to the washing steps. Images A, B and C are 50, 75 $\mu\text{l}$ Span and 50 $\mu\text{l}$ NP4 particles respectively.                                                                                                                                                                                                              | 34 |
| <i>Figure 13:</i> | Representation of the preparation system (vessel). (dr) is the vessel radius and (dz) is the length the sample travels within the vessel during the mixing process. These values in combination with the velocity and duration of mixing are used to calculate the energy used to achieve the emulsion in the system.                                                   | 36 |

- Figure 14:** Particle size distribution (PSD) the particles produced using the different emulsion parameters. The red (—▲—) peak indicates the 6  $\mu\text{m}$  particles followed by the green (—■—) peak for the 13  $\mu\text{m}$  and the blue (—◆—) peak for the 20  $\mu\text{m}$  particles. 38
- Figure 15:** A, B and C are dot plots of the 6  $\mu\text{m}$ , 13  $\mu\text{m}$  and 20  $\mu\text{m}$  particle populations respectively. P1 represents the sample population, P2 was sorted for microscopic analysis as it was considered representative of the population, P3 represents the more complex particles in the population and P4 represents the large or aggregated particles in the sample. 41
- Figure 16:** Microscopic images (P2 region of flow cytometry analysis) of the different particles produced and their size distribution. (A) Image of the 6  $\mu\text{m}$  sized particles (B) Image of the 13  $\mu\text{m}$  sized particles and (C) Image of the 20  $\mu\text{m}$  sized particles. (600x magnification). 43
- Figure 17:** Light microscopy image of undyed ReSyn™ particles using a 100x oil immersion objective (1000x magnification). 44
- Figure 18:** Images for particle density determination experimentation. 45
- Figure 19:** Absorbance spectra and chemical structures of the dyes used during experimentation. The blue, red and yellow curves represent RBBR, Congo Red and Brilliant Yellow respectively. The three dyes chosen have distinct spectral wavelength optima with limited overlap. 46

**Figure 20:** Particle dye binding capacity based on volume of individual particle sizes. 48

**Figure 21:** Dye binding of the different dyes per mass of particles dyed. Comparison of the dye binding capacities of the different particle sizes with different dyes. 49

**Figure 22:** Dye molecule structures, arrows indicate position of functional groups for binding. 50

**Figure 23:** Microscopic images of the different dyed particle preparations, showing the particles still retain their translucent property (1000x magnification). 52

| <b>Table</b>    | <b>Title</b>                                                                               | <b>Pg no.</b> |
|-----------------|--------------------------------------------------------------------------------------------|---------------|
| <b>Table 1:</b> | Summary of the concentrations of dye used for dyeing particles.                            | 32            |
| <b>Table 2:</b> | Measurements of energy input for the different manufacturing procedures.                   | 36            |
| <b>Table 3:</b> | Determination of particle yield by dry weight determination per starting raw material.     | 37            |
| <b>Table 4:</b> | Laser diffraction statistics of the different sample populations.                          | 38            |
| <b>Table 5:</b> | A comparison of the particle technologies currently available for diagnostic applications. | 54            |
| <b>Table 6:</b> | A comparison of the coloured microspheres used in applications other than diagnostics.     | 56            |



## LIST OF ABBREVIATIONS

|                                   |        |
|-----------------------------------|--------|
| Antigen                           | Ag     |
| Antibody                          | Ab     |
| Charged coupled device            | CCD    |
| Drug delivery systems             | DDS    |
| Enzyme-linked-immunosorbent assay | ELISA  |
| Gold nanoparticle                 | AuNP   |
| Hydrophilic-lipophilic balance    | HLB    |
| Hydrochloric Acid                 | HCl    |
| Lab-on-chip                       | LOC    |
| Lateral flow assays               | LFA    |
| Nonoxynol                         | NP4    |
| Polyethyleneimine                 | PEI    |
| Particle size distribution        | PSD    |
| Remazol Brilliant Blue R          | RBBR   |
| Sodium chloride                   | NaCl   |
| Ultra violet- visible             | UV-VIS |



## CHAPTER 1



# INTRODUCTION

## 1.1 BACKGROUND

The market for microparticles is constantly changing and expanding as the requirements for research and industry advance (Fenniri *et al.*, 2007). Current particle technologies are required to meet the progress being made for the different applications as well as to act as enabling technologies to assist in realising new applications and industries (Vignali, 2000). Well-defined polymer particles offer suitable supports for a large variety of biotechnological, pharmaceutical and medical applications (Pichot, 2004).

An example of an existing application includes particles of defined sizes ranging from 20 nm to 2000  $\mu\text{m}$  which are used as reference or calibration standards (whitehousescientific, 2009). Functionalised latex particles are currently used for immunoassays and rapid diagnostic tests (Andreotti *et al.*, 2003, Rundström *et al.*, 2007, Franse *et al.*, 2008 & Posthuma-Trumpie *et al.*, 2009), detection agents for enzyme-linked immunosorbent assay (ELISA) (Sato *et al.*, 2000), flow cytometry (Schwartz *et al.*, 1998), and charged/functionalised particles for protein or enzyme immobilisation (Cakmak *et al.*, 2009) or delivery systems for food and pharmaceutical applications (Stejskal *et al.*, 2000, Zhang *et al.*, 2007 & Rong-Hwa *et al.*, 2010).

Improvements in immunoassay performance have concentrated on developing particulate systems with improved properties (Seydack, 2005). These include the preparation of microparticles with enhanced visibility and colour discrimination (Yates *et al.*, 2000). These detection agents may be dyed using fluorophores, chromophores, fluorochromes or scintillators (Bangs *et al.*, 1994). Advancements in immunoassay technologies have resulted in the ability to develop simultaneous detection methods of multiple analytes (multiplexing) (Müller *et al.*, 1997), detectable labels for measuring analytes (Camilla *et al.*, 2001), optical properties for enhanced detection with or without the use of instrumentation, and the ability to discriminate the signal from

potential background interference in the case of detection with instrumentation (Mercolino *et al.*, 1994).

Market leaders in microparticle technology have demonstrated as much as 25% dye loading by weight (thermoscientific,2009). These microspheres are designed for application in research and the development of lateral flow diagnostic tests, where labelling and detection of low sample (analyte) concentrations is required (Nolan *et al.*, 2006). Dyed reagent microspheres with higher dye intensity provide enhanced test sensitivity in qualitative and quantitative lateral flow tests (Bangs labs tech note 301).

Increased sensitivity can be achieved through the use of multicoloured and/or increased detection agent load, e.g. increased dye load or alternate improved detection properties such as improved chromophores (Tozzoli *et al.*, 2007). New labels and detection systems that are capable of multiplexing, which can be used in miniaturized (micro and nano scale) platforms are becoming important for bio-analysis (Penn *et al.*, 2003).

Sensitive methods that allow identification of biomolecules at earlier disease states provide better prospects for effective therapy and better health (Agasti *et al.*, 2009). These particles have the potential to confer better sensitivity and signal amplification through preparation of particles with improved properties (Carville, 2007).

The nature of the particle used for the different applications must satisfy specific criteria. The density, charge and functionality are critical for their successful application of particles as detection reagents (Kawaguchi, 2000). The size of the microparticle influences the available surface area for binding and light scattering properties (Rosi *et al.*, 2005). The uniformity or monodispersity of the microparticles used are important for giving reliable and reproducible results for an intended application (Martín-Banderas *et al.*, 2006). Uniformity is not limited to the size but extends to other properties such as the chemistry and morphology (Kawaguchi, 2000). The charge on

the particles is critical for the prevention of aggregation and to reduce the non-specific binding of biologicals to its surface (Rembaum *et al.*, 1976).

## **1.2 PROBLEM STATEMENT**

In general, current limitations associated with microparticle technologies include, limited surface area (limited binding area), sensitivity (detection requires a lot of analyte to bind), non specific binding, stability of bound molecules and expense (Fenniri *et al.*, 2007). Particle technologies under development need to overcome the current limitations without compromising on known advantageous properties such as narrow size distribution and chemical functionality (Seydack, 2005).

## **1.3 AIM**

Due to the variety of applications of chromophoric particles, this study intends to evaluate the ReSyn™ technology as a potential candidate for inclusion in the aforementioned applications. Of interest is the suitability of the particles as research and diagnostic detection agents. The intention is to achieve this by investigating the effect of various emulsion modifications to determine the effect on particle size since particle size distribution is a key component for determining the breadth of feasible applications. Others parameters under consideration include optical, density and dye loading capacity of the microparticles.

## **CHAPTER 2**

### **Literature Review**



## 2.1 Applications of microparticles

### 2.1.1 Diagnostic detection agents

Diagnostic tests and assays make use of sub-micron sized latex particles and colloidal gold nanoparticles (AuNP) as detection agents for immunologically based reactions (Bangs labs tech note 303 & Bonenberger *et al.*, 2006). Bead based diagnostic assays utilising these particles include; agglutination tests (latex), particle capture assays, particle immunoassays and dyed particle sandwich ELISA tests (Bangs *et al.*, 1994).

Diagnostic applications, such as lateral flow assays (LFA) combine immunoassay principles with thin layer and paper chromatography, based on fluid migration (Figure 1) (Posthuma-Trumpie *et al.*, 2009). Coloured latex or colloidal gold particles are widely used as detection labels in LFA's and colloidal gold is currently used as the primary detection particle (Ling *et al.*, 2009). The major advantage of using colloidal gold for diagnostic detection is the improved flow properties and detectability (Shyu, *et al.*, 2002). Latex particles can be dyed to achieve a variety of colours, providing more versatile visual and optical detection capabilities than colloidal gold which is limited to a single colour (pink). This enables detection of more than one parameter at a time (Yguerabide, *et al.*, 2001).

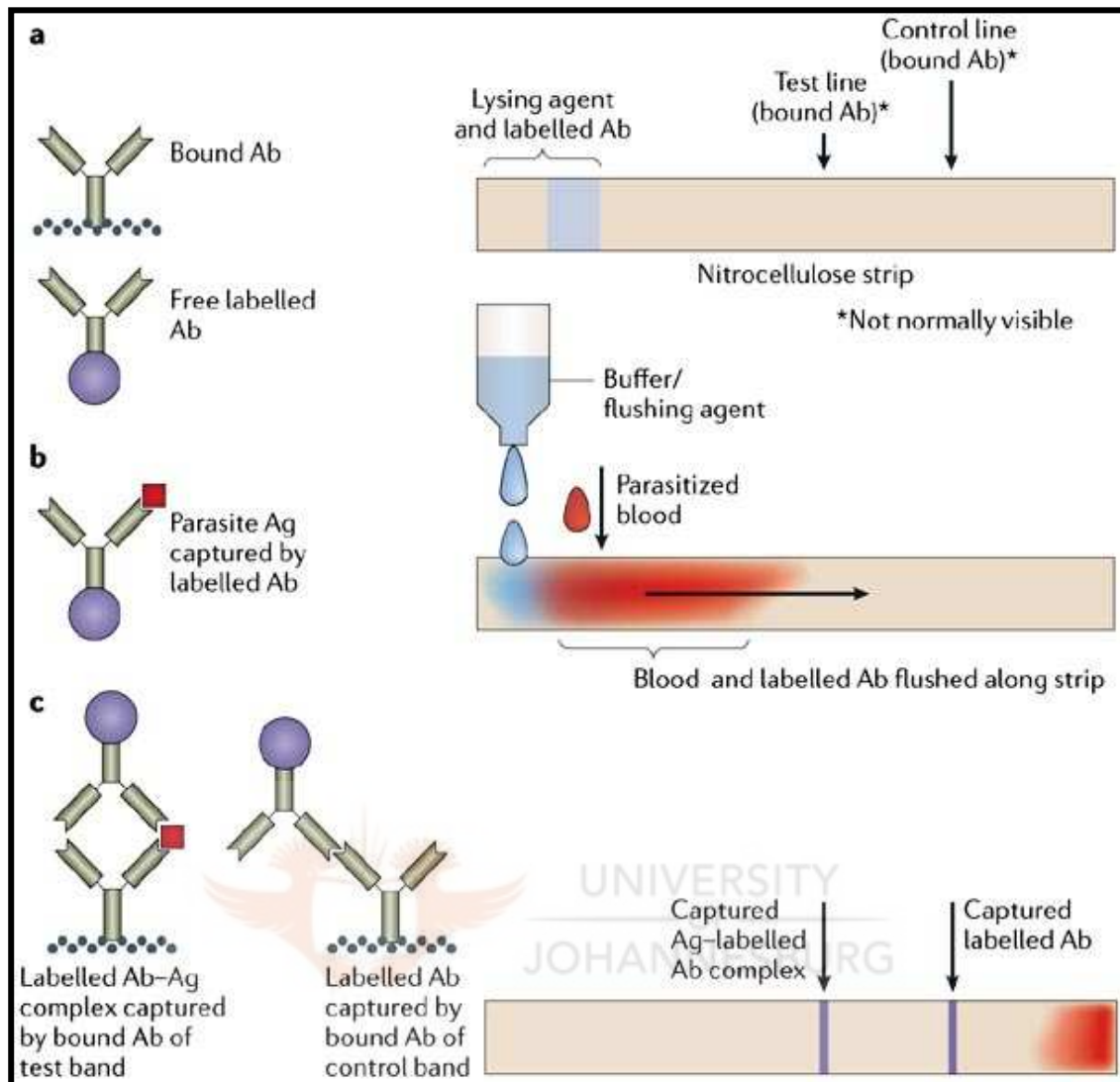


**Figure 1:** Representation demonstrating the principle of lateral flow assay technology. (a) Free Ab used as a control and an antibody specific to the antigen of interest is bound to coloured microparticles used as detection agents. (b) Conjugation of antigen with antibody bound microparticles followed by migration to the test line. (c) Reaction of Ab-Ag conjugates with another Ab at the test line as well as binding of free Ab in the control line (reproduced from Bell *et al.*, 2006).

An immunoassay is often based on the 'sandwich' format which uses two antibodies of distinct specificities. In the case of lateral flow immunoassays (Figure 1), one antibody is immobilized to a defined detection region (test line) on a porous membrane, while the other antibody is conjugated to the detection agent (colloidal gold or coloured latex particles). The biological sample containing the potential antigen is added to the membrane and allowed to react with the antibody-coated particles (detection agent). The conjugate then migrates along the porous membrane by capillary action over



the detection line, which in turn binds the antigen and prevents further migration of the particles. This results in accumulation of the coloured particles resulting in a distinct change of colour in the test line (Figure 2b). The colour intensity of the line is proportional to the antigen concentration in the biological sample (Figure 2). In the absence of the analyte, no gold or latex particles bind to the second antibody in the test line. The control line is designed to ensure the validity of the test and should always be positive to indicate the test is working (Figure 2b &c).

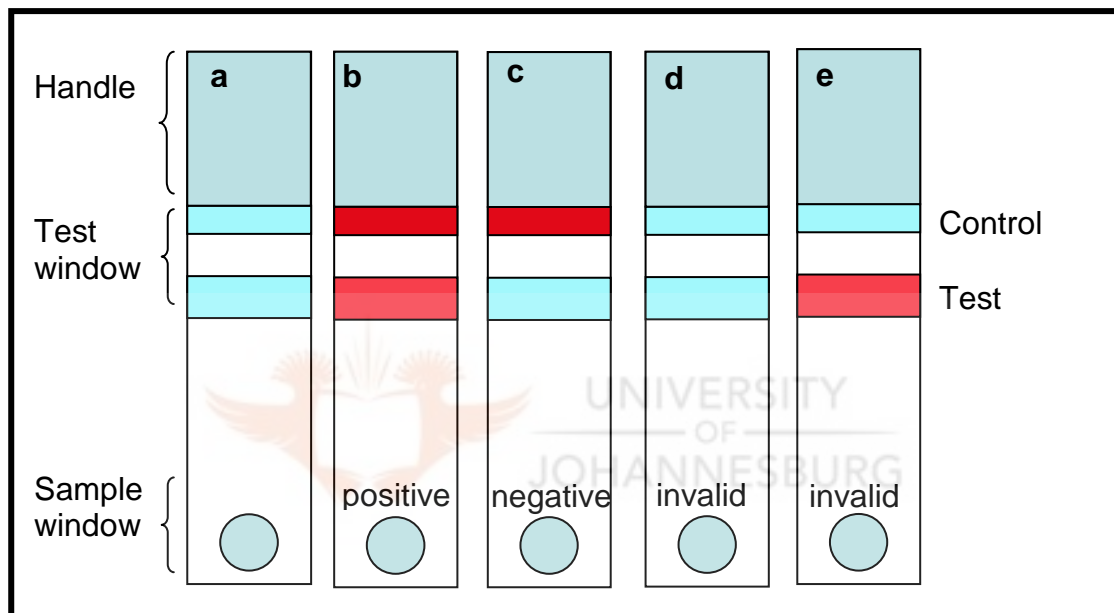


**Figure 2:** A typical rapid diagnostic test and the interpretation of the results. (a) Test strip before the application of sample, no distinct colour is visible. (b) Positive result, change in colour in the test and control region. Distinct and consistent colour bands appear on the control and test regions. Colour intensity of the bands may vary according to concentration of Ag of interest. (c) Negative result only one line appears in the control region. (d) Invalid test, no line appears in the control or test region. (e) Invalid test when the test line changes colour while the control line does not.

Immunoassays utilising gold nanoparticles require good labelling efficiency, i.e. good interaction between the particle and the antibody, with a good particle size for visibility (Dendukuri *et al.*, 2009). Developments towards improving gold nanoparticles as detection agents with improved optical properties for increased sensitivity are ongoing (Baptista *et al.*, 2008 & Sanvicens, *et al.*, 2008). Research by Lui *et al.*, (2010) focused on methods of particle preparation with the aim of producing particles with increased uniformity and lower density. These properties are associated with the sensitivity of the intended application including flow and visibility.

The aim of optimising colloidal gold preparation methods is to achieve 'good' colloidal gold. The uniformity of the colloidal gold influences the aggregation, stability and optical properties of the particles (Yeh *et al.*, 2009). An example of improving the sensitivity of colloidal gold by altering the optical properties can be found in a study by Rong-Hwa *et al.* (2010), where inclusion of silver improved the visual properties of the colloidal gold and hence its sensitivity. Gold nanoparticles catalyze the reduction of silver and thus act as nuclei for silver deposition, resulting in improved colour development to intensify the binding signal of the colloidal gold at the test line (Newman *et al.*, 1999).

The requirements for improved sensitivity of LFA's have led to the development of signal enhancing steps. For example Choi *et al.*, (2010) developed a dual system for LFA composed of two AuNP-antibody conjugates (Figure 3). The 1<sup>st</sup> AuNP conjugate was prepared and conjugated to an Ab as part of the sandwich assay, the 2<sup>nd</sup> AuNP conjugate was larger in size and was designed to bind to the 1<sup>st</sup> AuNP. The two nanoparticles were positioned at different points in the diagnostic test strip to prevent interaction before application of sample. This double conjugate assay improved the sensitivity of the LFA for troponin I.

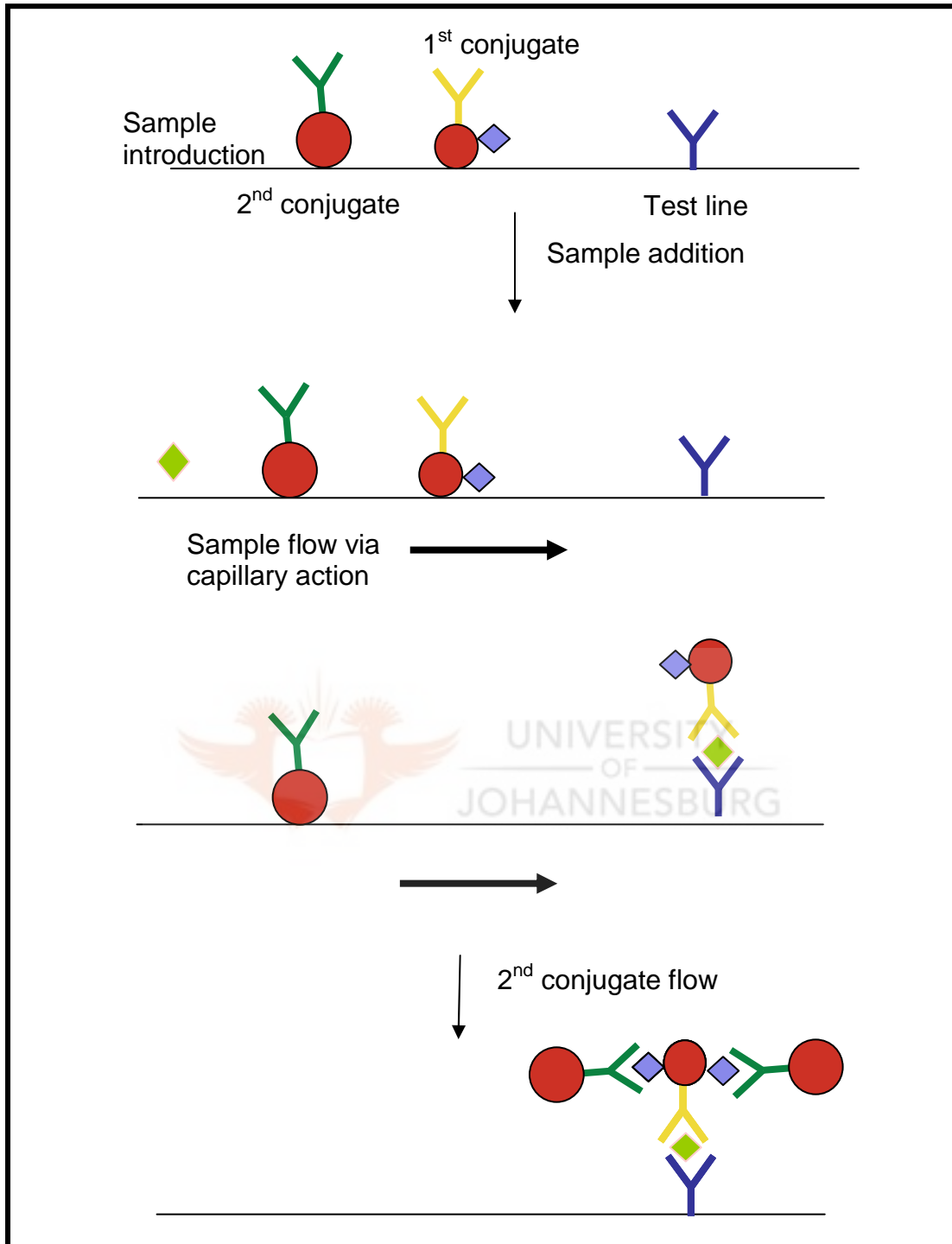


**Figure 3:** Improving signal amplification for lateral flow diagnostic using dual AuNP system. The 1<sup>st</sup> AuNP is conjugated with the Ab specific for the analyte of interest and blocked with BSA. The 2<sup>nd</sup> AuNP is conjugated with anti-BSA Ab to bind specifically with the 1<sup>st</sup> AuNP conjugate to amplify the signal generated from the 1<sup>st</sup> AuNP.

### 2.1.2 Research detection agents

Microparticle properties can be exploited for different research applications (Warsinke *et al.*, 2009). In cell labelling studies the distinct optical properties of microparticles can be used to provide and or generate contrast in tissue samples (Chithrani *et al.*, 2006). Microparticles with distinct optical properties such as colloidal gold can be functionalised for attachment to specific biological tissues and are suitable for visualisation applications (Figure 4) (Sperling *et al.*, 2008).

Labelling of tissue samples for electron microscope studies with gold particles (Figure 5) ensures the label is not easily mistaken for a tissue structure. The resolution of this labelling in electron microscopy is thus higher than alternate (Chu *et al.*, 2005). Cell labelling studies for microscopic analysis utilise microparticles that are biocompatible, in the size range of 0.001-0.4  $\mu\text{m}$  in diameter and have functional groups that allow for covalent binding of antibodies or other biomolecules with affinity for their target (Rembaum *et al.*, 1976 & Gosh *et al.*, 2008).

In a study by Chithrani *et al.*, (2006) HeLa hepatocytes were exposed to gold nanoparticles to evaluate biological uptake. Transmission electron microscopy of labelled tissue indicated that the particles were efficiently translocated into the cells and were easily distinguishable from the surrounding tissue. This demonstrated that the unique optical properties of gold nanoparticles can be used for specific applications and can be easily detected. Their translocation into the cells alludes to their application as drug delivery systems (DDS).

AuNP have the potential to act as contrast agents in reflectance based optical imaging (Figure 5). This arises from their unique optical response to light which allows them to absorb and scatter light. The optical signal generated can be further enhanced through aggregation or localisation of AuNP (Stirhoff *et al.*, 2000 & Kah *et al.*, 2008).

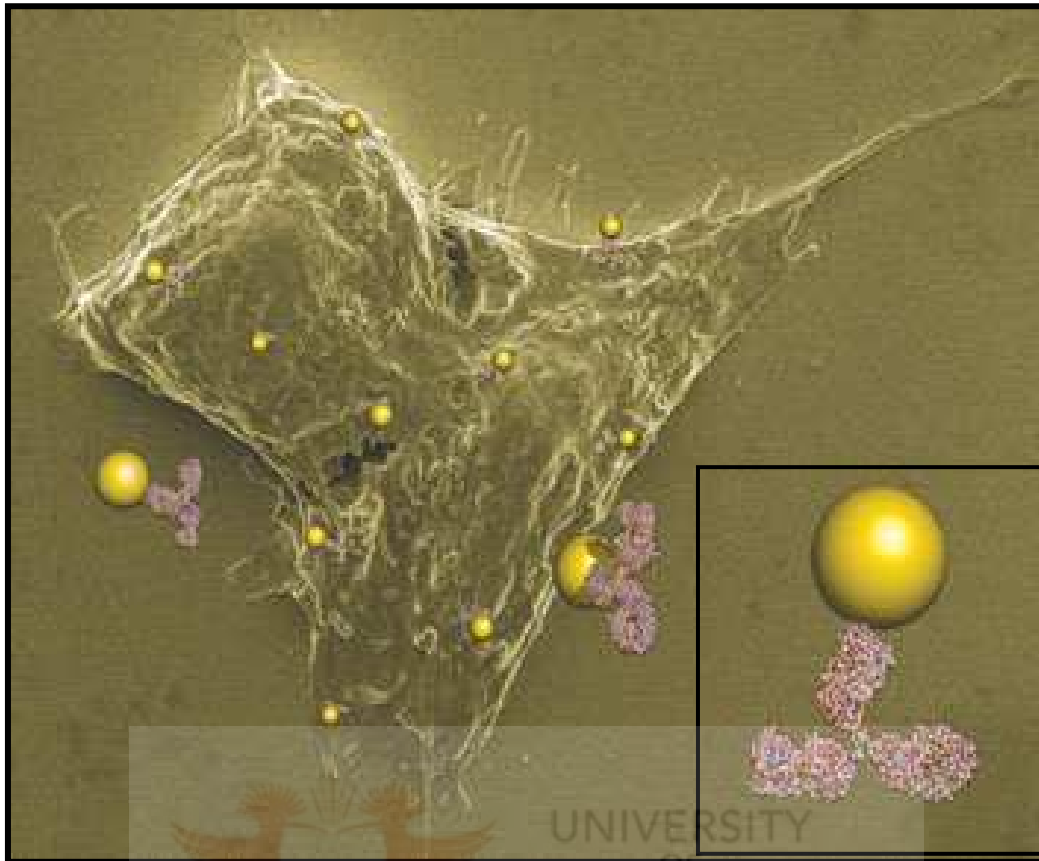


**Figure 4:** Scheme indicating application of AuNP as contrast agents (not drawn to scale, AuNP (~10-40nm), DNA (~60kDa) and or proteins (~20-30kDa). The AuNP allow the labelling of the cell or parts of the cell for visualisation. The insert shows a AuNP that has been functionalised with an Ab adsorbed to its surface and used as a contrast agent and targeted delivery and or attachment of biomolecules (reproduced from Sperling *et al.*, 2008).

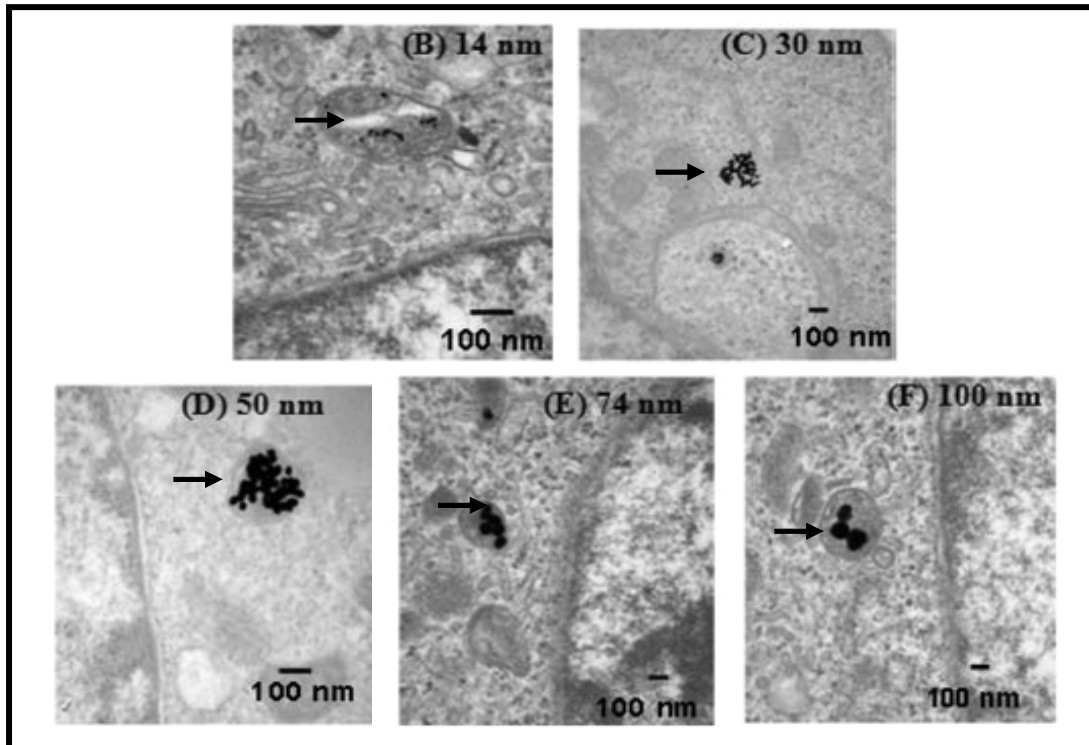


**Figure 5:** TEM images of AuNP of various sizes trapped inside vesicles of HeLa cells. Images B- F are AuNP with sizes 14, 30, 50, 74 and 100 nm respectively, gold particles are used as contrast agents (reproduced from Chithrani *et al.*, 2006).

### 2.1.3 Detection agents for flow cytometry

Flow cytometry uses the principles of light scattering, light excitation and emission of fluorochromes, to generate specific multi-parameter data from particles and cells (Kellar *et al.*, 2002). It is a technique that is used to quantify as well as provide qualitative data of sample populations. It is used in analysing expression of cell surface and intracellular molecules, characterizing and defining different cell types in heterogeneous cell populations, assessing the purity of isolated subpopulations, and analyzing cell size and volume (Brown *et al.*, 2000). Its use is not only limited to biological applications, synthetic molecules such as polymer beads have also been studied using this technique (Spherotech, 2009,).

Flow cytometry is now a widely used technique for it is predominantly used to measure fluorescence intensity produced by fluorescent-labelled biomolecules (BD Biosciences, 2000). Beads of the same size are labelled with the same fluorophore but different intensities (Brookhaven, 2009). Figure 6 each bead is coupled to a unique antibody or probe that recognizes a specific molecule after the beads are mixed with a sample. The beads are ordered into a stream of single particles through hydrodynamic flow focusing. The "sheath" fluid surrounds a thin core thread of sample and flows at a higher speed than sample stream. This spaces the cells out so that only one passes the laser beam at a time, and keeps the cells centred in the flowing stream so that they pass the laser beam optimally centred. The sample stream and sheath fluid do not mix and thus laminar flow occurs. Laser beams are used to decode the beads and quantify the fluorescence, as well as the forward and side scatter light emitted from the particles. The combination of scattered and fluorescent light is detected and analyzed. Forward scatter correlates with the size and side scatter measures the complexity of the particle. Fluorochromes used for detection/staining will emit light when excited by a laser with the corresponding excitation wavelength (Joos *et al.*, 2002).

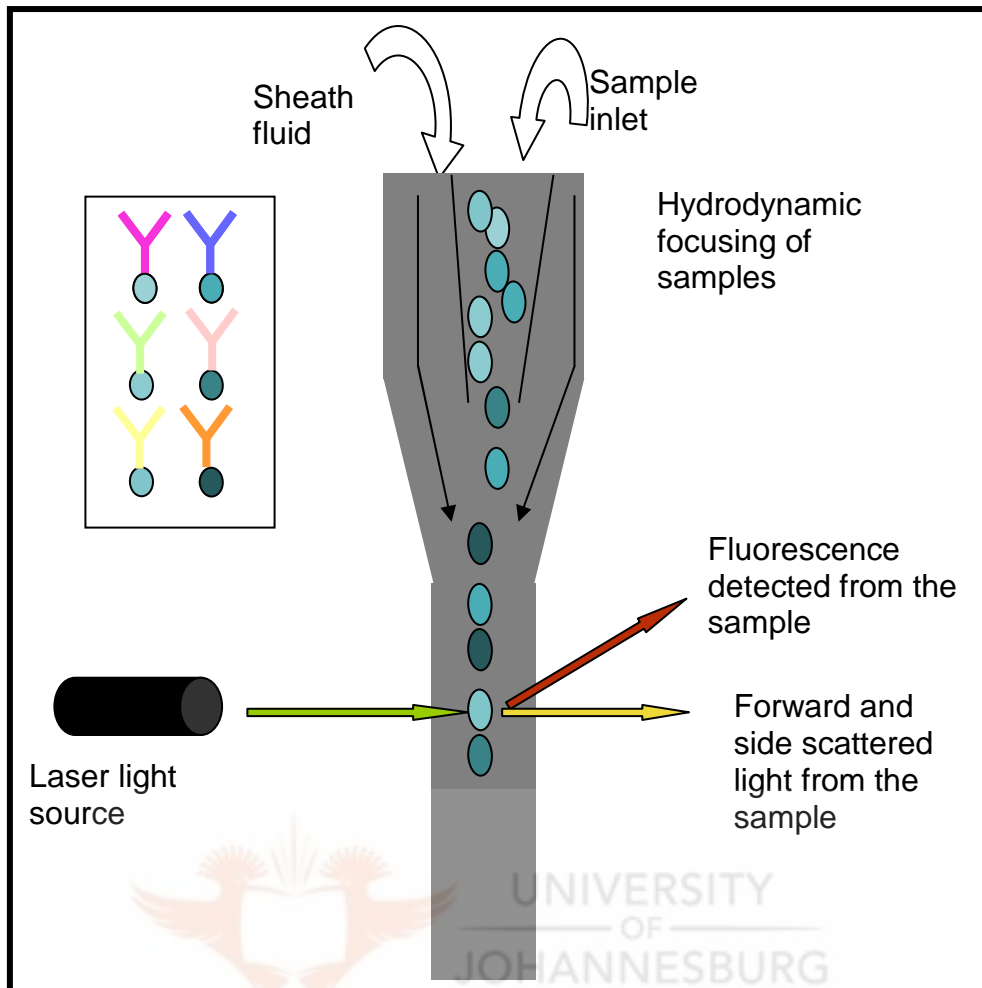


**Figure 6:** Diagram showing how the bead-based flow cytometric technology operates. When the sample in suspension buffer is run through the cytometer, it is hydrodynamically focused, using sheath fluid, through a small nozzle. The tiny 'stream' of fluid takes the particles past the laser light one bead at a time. There are a number of detectors to detect the light scattered from the particles as they go through the beam. The insert shows beads of the same size with different intensities of the same fluorophore and functionalised for specific binding

Camilla *et al.*, (2001) demonstrated a specific and quantitative immunoassay through the combined use of flow cytometry and latex microparticles of specific sizes. Bead based flow cytometry assays need to meet the following criteria of specificity (binding to specific biomolecules), sensitivity (detection of low abundance of biomolecules), simplicity (basic skills required for operating and or performing assays), reliability (to ensure reproducible results), multiplex capabilities (allowing for complex sample analysis) (Vignali, 2000 & Holmes *et al.*, 2007).



Multiplexing beads offer several advantages over single target detection methods; less time and cost per analysis, simpler protocol formats, fewer sample volumes required and reproducible and reliable measurements (Tozzoli *et al.*, 2007 & Derveaux *et al.*, 2008). Ten intensities of two colours enable the encoding of  $10^2$  different microspheres that can be discriminated by a flow cytometer (Nolan *et al.*, 2006). The beads are coded using unique tags, chromophores or fluorophores (Figure 7) depending on the detection that is used. The unique coding designated to each particle affords easy identification and detection (Birtwell *et al.*, 2010).

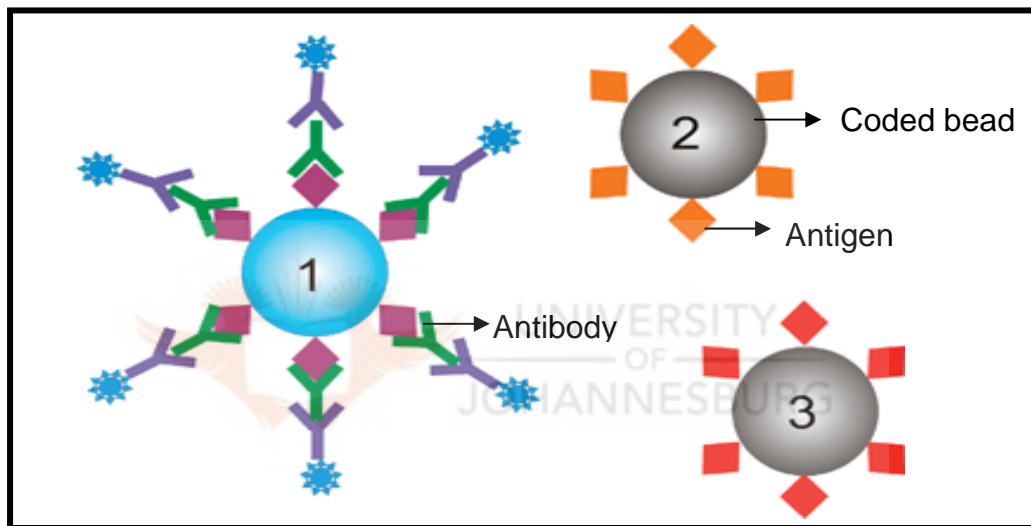


**Figure 7: Coded beads used in multiplex assays. The beads are coded with unique tags, chromophores or fluorophores for easy identification upon detection (reproduced from Birtwell *et al.*, 2010).**

Various systems have been formulated such as multiplexed suspension (bead—based) assays which offer a number of advantages over alternative approaches such as ELISAs and microarrays. Molecular sensitivities of bead based assays are comparable to both ELISAs and microarrays and are realistic candidates for high throughput, low sample volume replacements for these technologies (Birtwell *et al.*, 2010). Wu *et al.*, (2008) successfully prepared two-dye labelled polystyrene particles. By controlling and varying the dye concentrations they were able to obtain two distinguishable parts of fluorescence and varied intensities.

#### 2.1.4 Enzyme immobilisation

The major advantage of enzyme immobilization is that it facilitates recovery and recyclability of catalysts. The generally very expensive and valuable biocatalysts can be used repeatedly used in successive batches (Biro *et al.*, 2008). Enzymes are immobilized on solid supports having particle sizes ranging from tens of micrometers to several millimetres. Microparticles used have specific surface area with numerous active sites for the enzyme molecules to bind (González *et al.*, 2005). The supports used in immobilisation must offer stability and adsorption of enzymes with out leaching (Brady *et al.*, 2009). Microparticles provide increased surface to volume ratio reducing the volume of reagents required. Biomolecules can be immobilised on particle surfaces thus localising the chemistry to a defined point for rapid analysis (Lei *et al.*, 2002).

#### 2.1.5 Microfluidics

Microfluidics involves the processing and manipulation of small (microlitre and less) amounts of fluids in small channel dimensions (micrometer) (Whitesides, 2006), it takes advantage of the already advance microfabrication processes and technologies developed by the microelectro-mechanical systems industry (Xia *et al.*, 1998). It has the potential to impact many research fields including clinical diagnostic, chemistry, biochemistry, biosensing, immunology, genetic research, drug discovery and drug delivery (Whitesides *et al.*, 2001b). Systems and devices are being realised through microfluidics research by modernising and miniaturising existing techniques such as sample transport and detection (Beebe *et al.*, 2002). These processes can be developed for microfluidic platforms to perform better and more efficiently compared to currently available bench top technologies (Whitesides *et al.*, 2001a).

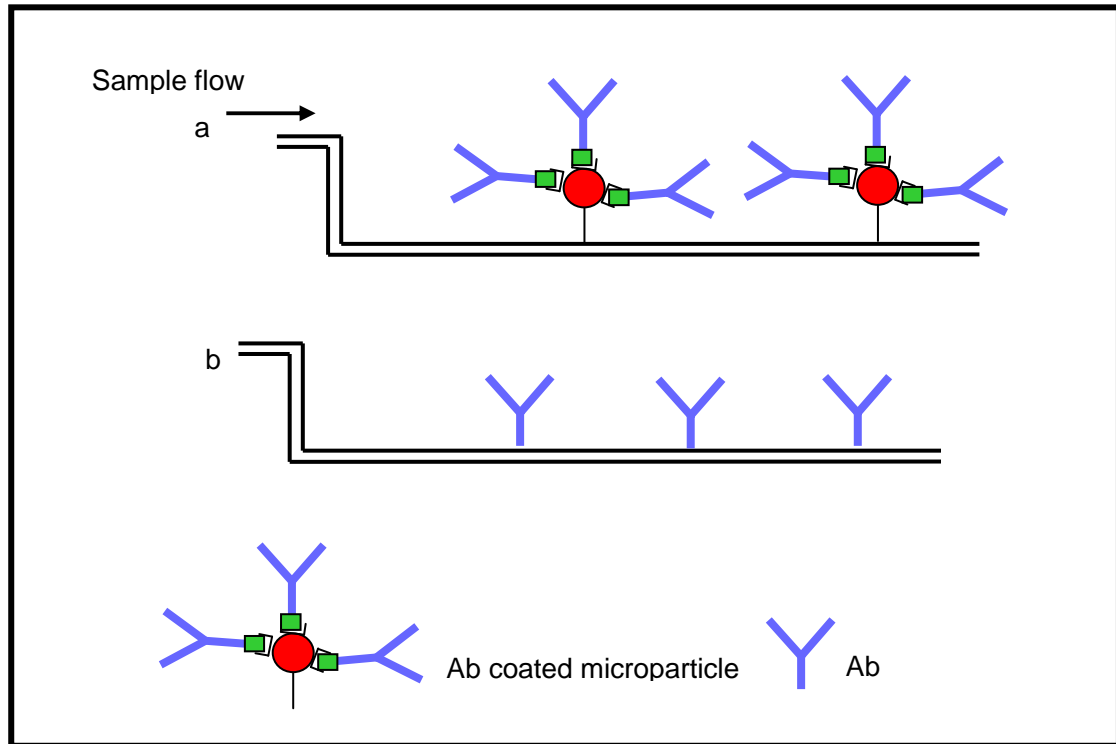


**Figure 8:** Micro channels (100 $\mu$ m) used in the development of miniaturised immunoassays. (a) Functionalised microparticles are conjugated to specific Ab and attached to the microchannel surface. The particles provide increased surface area for improved sensitivity. (b) Alternative limited sensitivity; Ab are attached directly onto the microchannel surface.

Microfluidic separation relies on the exploitation of particle properties to achieve the intended separation (Anderson *et al.*, 2003). The charge or magnetic properties of microparticles can be used for dielectrophoretic (DEP) or magnetic separation respectively (Yasukawa, *et al.*, 2007). A study by Kuntaegowdanahalli *et al.*, (2009) investigated the use of an inertial microfluidic system for passive simultaneous separation of microparticles of sizes 10, 15 and 20 $\mu$ m. The ability to sort these sizes has applications for high throughput sorting in medical and environmental industries.

Microfluidic bead-based immunoassays offer several advantages over the conventional counterparts (Bange *et al.*, 2005). They provide shorter operational times, wide range particle surface chemistries available, better specificity for target analyte, and ease of recovery (Murakami *et al.*, 2004). Miniaturised assays are accepted on the basis that they function similarly to other assays such as ELISA which are currently the gold standard. An

increase in sensitivity is achieved due to the increase in available surface area for binding (Figure 8), faster analysis times and a reduction in cost as well as ease of handling (Sivagnanam *et al.*, 2009). Unfortunately miniaturisation through microfluidics often occurs at the expense of detectability and instrumentation for detection. Particles with high dye loading capabilities can potentially address this limitation (Uchiyama *et al.*, 2004).

## 2.2 Factors influencing applications of microparticles

The market for microparticles is constantly changing and expanding as the requirements for research and industry advance (Fenniri *et al.*, 2007). Current particle technologies are required to meet the progress being made for the different applications as well as to act as enabling technologies to assist in realising new applications (Vignali, 2000).

Research has been dedicated to the design and preparation of particles with appropriate properties. These properties are conferred to the particles according to the intended application (Pichot, 2004). The properties of microparticles, such as their size, usually determines the available surface area for binding, while monodispersity is often required for applications such as diagnostics and can affect the reproducibility of the intended application (Park *et al.*, 2002); presence of bioreactive groups; biodegradability, bioresorbability and nontoxicity are required in the case of particles used as DDS (Pichot, 2004).

The optical properties can affect the application of particles as contrast agents, particularly for cell labelling studies (Yates *et al.*, 2000). The intensity of colour in the case of dyed particles can result in very high contrast and relative visibility to background materials, which can be observed directly in the media being tested either visually or by light microscopy (Dukescientific, 2009).

From this literature review it is evident that the development of microparticles with improved properties, such as better detection agents, increased dye loads and flow properties has the potential to overcome limitations in current technologies including limited detection, stability and surface area. Of particular interest is their application as diagnostic detection agents for point of care devices (Rundström et al., 2007).

### 2.3 ReSyn™ technology description

The ReSyn™ technology developed by Jordaan *et al.*, (2009) has several features that can be used to potentially overcome these current limitations and meet increasingly stringent industry and research requirements. ReSyn™ is a proprietary polymer matrix prepared using an emulsion based technique. The advantages of this technology include control of particle size. The advantages stem from the loosely linked polymer network. The loose network confers optical translucency, a property that can result in easier detection using optical measurements and detection techniques (Figure 9). The particles contain a high density of functional groups on the polymer strand network that are available for binding of biomolecules and/or chemicals through covalent, hydrophobic, affinity and ionic bonds.

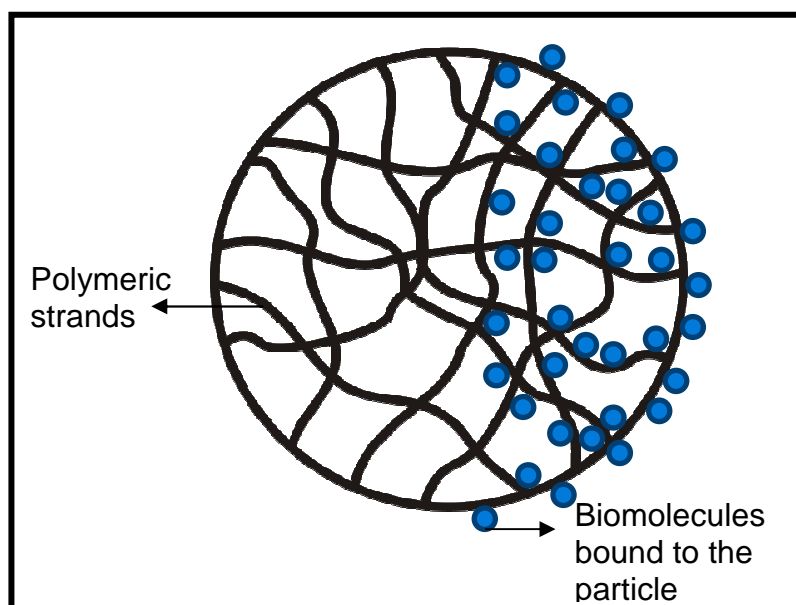


**Figure 9: Illustration of a ReSyn™ particle. The particles formed are spherical and contain a high density of functional groups.**

The following research investigated the preparation of microparticles of different sizes by changing reaction parameters. The particles were prepared with specific characteristics such as high dye loading capacity and enhanced optical properties for improved sensitivity as well as lower density.

## **2.4 Properties of microparticles**

### **2.4.1 Microparticle size distribution**

The controlling of microparticle size through physical properties of the materials, such as polymer and surfactant concentration (Gurkov *et al.*, 1994 & Biro *et al.*, 2009) and through modifying the experimental conditions (Mitragotri *et al.*, 2008) is of interest.

Emulsion based particle synthesis uses an aqueous reaction media. An emulsion system is formed of at least three components. These are the oil phase, the water phase and the surface-active agent. The physicochemical properties of these components affect the emulsion behaviour (Salager *et al.*, 1996 and van Zyl *et al.*, 2004). During emulsification, a combination of surface active agent and agitation, are used. The nature of such an emulsion is then determined by the affinity of the surface active agent whether it is towards the water or oil phase (Sajjadi *et al.*, 2003). The physiochemical formulation of the emulsion system is sometimes more important than the surfactants, energy and stirring/mixing parameters individually (Salager *et al.*, 1996).

A study by Lui *et al.*, (2005) investigated changes in the emulsion microstructure and stability by varying the amount of energy delivered during formulation. They observed the role that energy input plays but also indicated the role of the physiochemical conditions of the emulsion components to greatly influence the outcome. For the samples prepared with low concentrations of surfactant a significant increase in droplet size was achieved to that of the high surfactant concentration.

#### 2.4.1.1 Surfactants

In the preparation of polymer particles the size and morphology are primarily dependent on two factors, the concentration and type of surfactants used (Jang *et al.*, 2002) and the energy delivered during formulation (Lui *et al.*, 2005). The surface active agent or emulsifier is an essential element for the initial formation and the long-term stability of emulsions (Gullapalli *et al.*, 1999). The general rule is that particle size can necessarily be reduced by increasing the surfactant concentration, resulting in a decrease in interfacial energy, and increased dispersion of the emulsion droplets (Lee *et al.*, 2005). Surfactants are used as emulsifiers in the food, cosmetic and pharmaceutical industries for the formulation of emulsions.

Surfactants contain an ionic head and a non-polar hydrocarbon tail (Figure 10) and upon dissolution the surfactant molecules align under critical micelle concentration (Hicks, 1971). The surfactants form micelles, which are required for particle formation by micellar nucleation. Additionally, the surfactants provide colloidal stability for the monomer droplets by forming a film around the suspending dispersed phase droplets. Strengthening of this film through concreting at the interface attains a much greater degree of the droplet stability (Antonietti, *et al.*, 1992 and Gullapalli *et al.*, 1999).

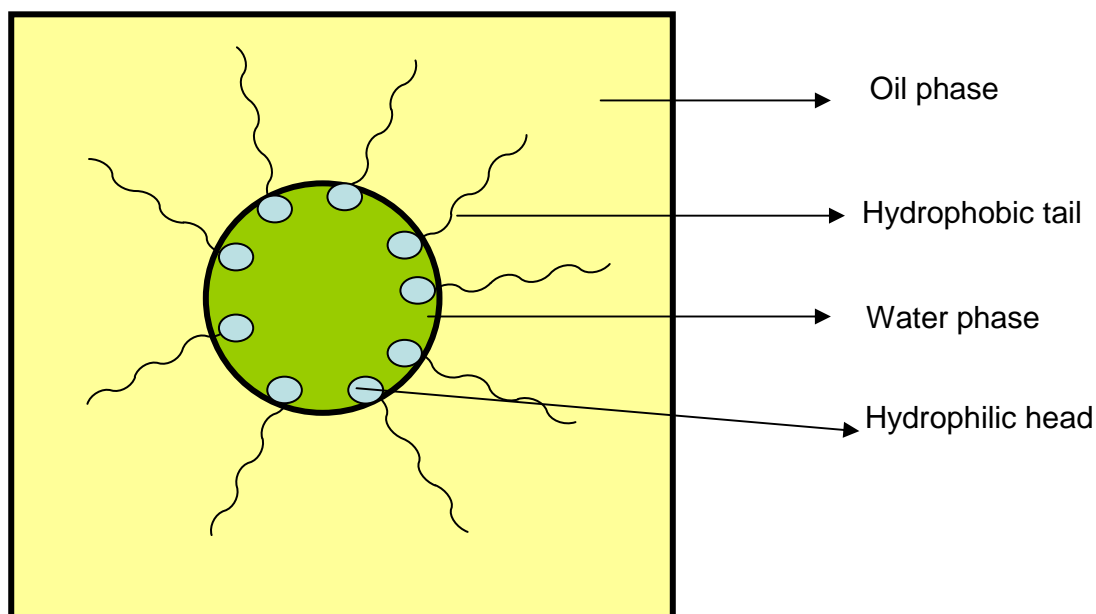


**Figure 10: Alignment of surfactant molecules during emulsification to form stable emulsion droplets. The hydrophobic tails orientate themselves and give stability to the formed emulsion droplets.**

The hydrophobic-lipophilic balance (HLB) factor for the different surfactants is an important parameter for emulsification as it directly influences the emulsion formation (Sajjadi *et al.*, 2003). The detergent is selected for an application based on this HLB as it indicates the suitability for emulsification of the emulsion components (Velev *et al.*, 1994). Examples of surfactants used for emulsion derived microparticles include Nonoxynol 4, Span and Tween. Nonoxynol 4 has an HLB factor of 8.9. Span, having an HLB factor of 8.6, is a more lipophilic surfactant and tends to be soluble in the oil phase (Gullapalli *et al.*, 1999).

The surfactant affinity to either the oil or water phase depends on other conditions such as the type of oil phase, the surfactant concentration and on the presence of other additives in the system (Sajjadi *et al.*, 2003). Tai *et al.*, (2001) has shown and emphasised the importance of taking into consideration the system HLB instead of the surfactant HLB factor only. The nature of the oil phase used can modify the geometry of the surfactant at the interface and thus affect the emulsion type and stability of the emulsion.



#### 2.4.1.2 Energy impact on emulsification

Emulsions are thermodynamically unstable and require energy during their formation. Mechanical energy in the form of (agitation or mixing) is the primary form of energy for emulsion formation (Campbell, 1991). Liu *et al.*, (2005), observed the role the energy input plays but also indicated the role of the physiochemical conditions of the emulsions to have a greatly influence the PSD of an emulsion.

#### 2.4.2 Optical properties of microparticles

Chromophoric and/or fluorescent particles have a broad range of applications. Of particular interest is their application as diagnostic detection agents for point of care devices (Rundström *et al.*, 2007). Pregnancy tests (Chard, 1992), food tests (Rong-Hwa *et al.*, 2010), lateral flow assays (Andreotti *et al.*, 2003) immunosorbent assays (Sato *et al.*, 2000) fluorescent labelling (Müller *et al.*, 1997) and microsphere based flow cytometric assays (Camilla *et al.*, 2001) all utilise labelled microparticles.

Solid supports used in applications as diagnostic detection agents require enhanced sensitivity, selectivity, mobility, and stability. Depending on the nature of the signal, the reactants may be detected visually, electronically, chemically, or physically (Andreotti *et al.*, 2003 & Agasti *et al.*, 2009). Areas that still require improvement have been identified, these include improved/simpler methods of preparation, improved size uniformity and the capacity to retain their properties, i.e. optical characteristics (Gañán-Calvo *et al.*, 2006).

The optical properties of ReSyn™ particles offer distinct advantages for their application as detection agents. They are optically translucent due to the loose polymer network. The high density of binding sites can be used to prepare microparticles with improved dye loads.

## 2.5 Objectives

The objectives of this research were:

- To manufacture polymer particles of 5, 10 and 20 microns in diameter by altering preparation parameters. To control particle size for determining the versatility of the technology for various particle-based applications.
- To evaluate the dye binding capacity of ReSyn™ particles by determining the amount of dye that can be incorporated in the particles.
- To investigate the physical properties such as density, size, morphology as well as optical characteristics.
- To compare ReSyn™ technology to the existing microparticle technologies with respect to the parameters of interest such as dye binding capacity and size.



## CHAPTER 3



### 3.1 Particle preparation

Particles were produced using a water-in-oil bi-emulsion process (Figure 11) as described previously (Jordaan *et al.*, 2009). In brief, two separate oil phases were prepared by dissolving 50  $\mu$ l NP4 detergent in 5ml of mineral oil. The mineral oil and detergent were mixed using a vortex (IKA<sup>®</sup>) at maximum speed (2500 rpm) for 10 seconds. To the one oil phase a water phase consisting of 200  $\mu$ l of 10 % polyethyleneimine (PEI) solution (pH adjusted to 9 using HCl) was added, and to the second 200  $\mu$ l of 20 % Glutaraldehyde (Grade II). These were subsequently emulsified using a vortex at maximum speed (2500 rpm) for 10 sec. The two emulsions were combined and mixed end-over-end at 60 rpm for 60 min to allow particle crosslinking to occur.

The particles were recovered by centrifugation at 3901x g for 5 min. The particles were subsequently washed six times using 50 ml MilliQ water (Millipore) to remove oil and detergent. The particles were stored at 4°C in a 20% ethanol solution until required. This method has been demonstrated to produce particles with an average size of 6  $\mu$ m (Jordaan *et al.*, 2009).

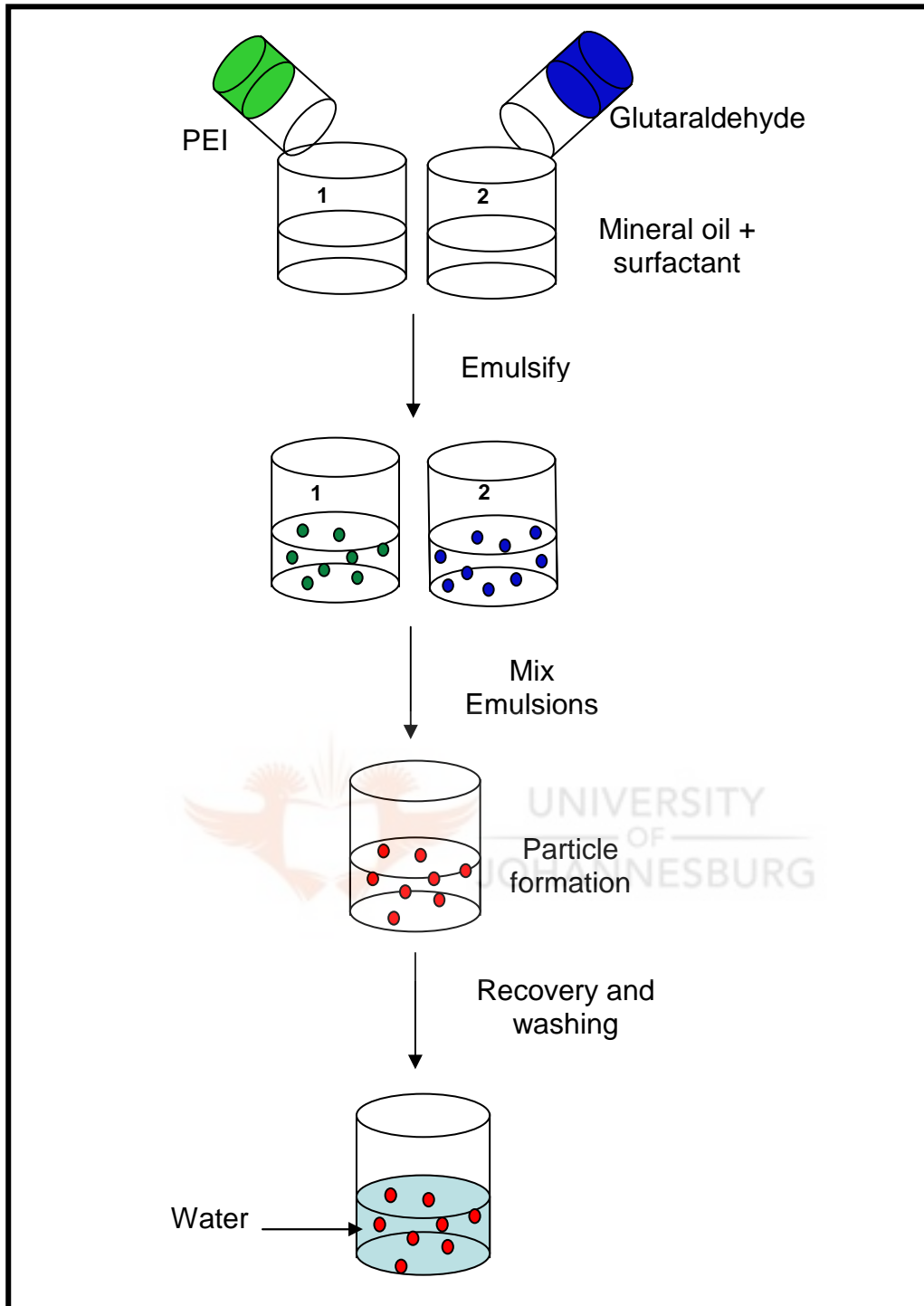


Figure 11: The particle preparation process as described in 3.1

### **3.2 Evaluation of emulsion parameters for particle size differentiation**

The manufacturing procedure as described in section 2.3.1 for the production of 6  $\mu\text{m}$  particles was modified for the manufacturing of 13  $\mu\text{m}$  and 20  $\mu\text{m}$  sized particles. The surfactant NP4 was substituted with 50  $\mu\text{l}$  and 75  $\mu\text{l}$  of Span 20 for the 13 and 20  $\mu\text{m}$  particles respectively. Magnetic stirring at 700 rpm for 25 sec was used for preparing the oil phase. The water phases remained the same as previously stated in section 2.3.1 and emulsified using a magnetic stirrer at 700 rpm for 25 seconds. The particles were recovered by centrifugation at 3901x g for 10 minutes. The particles were washed using 3x 50 ml aqueous solution of Triton®X100 (0.1%) followed by 10x 50 ml washes with MilliQ water. The particles were stored at 4°C in a 20% ethanol solution.

### **3.3 Particle Analysis**



#### **3.3.1 Particle Yield**

The samples were washed a minimum of three times using water to remove ethanol (recovery using 12470x g for 5 min). The pellet was subsequently made up to 5 ml using distilled water. Samples (1 ml) were lyophilised using Labconco Triad system and weighed to determine particle dry weight. Particle preparation and dry weight determination were performed in triplicate.

#### **3.3.2 Particle size distribution**

Particle size distribution (PSD) analysis was undertaken to determine the effect of the above mentioned variations in the emulsion parameters. Particles (1 ml) suspended in 20% ethanol were analysed using a Malvern Mastersizer 2000 using three different conditions, no sonication, pre-sonication (1 min) and in-line sonication. Samples were analysed in triplicate. Ultrasonication (pre- and in-line) can separate potential aggregates.

### **3.3.3 Flow Cytometry**

The particle sizes from the different preparation methods were evaluated using flow cytometry. Flow cytometric analysis of the particles was undertaken in the Central Analytical Facility of the Department of Physiology at Stellenbosch University by Dr. Ben Loos. The BD FACSAria and BD FACSDiva software was used to record the data and analyse the forward scatter (size) and side scatter (complexity) of the samples.

### **3.3.4 Microscopic analysis**

Microscopic analysis of the particles was undertaken using the Olympus Cell<sup>^</sup>R system attached to an IX81 Inverted fluorescence microscope equipped with a F-view-II cooled CCD camera (Soft Imaging Systems) with a Xenon-Arc burner (Olympus Biosystems GMBH) as the light source. Images were acquired using a 360 nm, 472 nm or 572 nm excitation filter. Emission images were collected using a UBG triple-bandpass emission filter cube (Chroma). Images were acquired using an Olympus Plan Apo N60x/1.4 Oil objective.

The morphology of native ReSyn<sup>™</sup> microparticles was characterised using light and fluorescence microscopy. Microscopic images were taken using the Olympus BX 41 light microscope with 1000x magnification using an oil immersion objective.

### **3.3.5 Particle density determination**

The approximate density of particle preparations was calculated using sucrose concentrations of known densities. Sucrose concentrations of 0, 1, 2, 4, 10, 12 and 14% were prepared. Samples of 50  $\mu$ l of particles were applied to 1 ml of sucrose solution and allowed to settle for 5 min. Polystyrene particles of known density,  $1.05 \text{ g.cm}^{-3}$ , were used as a control to validate the method.

### 3.4 Particle Dyeing

#### 3.4.1 Dyeing of ReSyn™ particles

The dyeing method used for the particles manufactured in chapter 2 section 2.1 and 2.2 was adapted from Compton *et al.*, (2002). Dye solutions were prepared consisting of 10 mg dye in 1 ml of water. Table 1 summarises the different dye concentrations used for dyeing the particle preparations. Dye solution (200 µl) was added to 800 µl of particle sample and heated at 70°C for 30 min shaking at 5 min intervals to avoid settling of the particles. The dyed particles were washed with 1ml distilled water from the milliQ water (Millipore) system until all the dye was removed. The particles were recovered by centrifugation at 12470x g for 3 min. The supernatants from all the washing steps were stored for absorption spectroscopy analysis.

#### 3.4.2 Evaluation of dye-particle interactions

Twenty seven dyes were screened to evaluate the capability of ReSyn™ particles to bind dyes. Only 20 of the dyes screened are represented in appendix 2 as 4 of the dyes did not dissolve using the preparation method described in section 3.4.1. Three of the dye samples changed colour properties after addition to the particles. Thus the evaluation of these does was not pursued further and investigation of this phenomenon was not explored further as it fell outside the scope of this study. Stringent elution processes were used to evaluate particle-dye interactions using NaCl (ionic), ethanol (hydrophobic) and chloroform (non-polar). Three major colours namely; blue, red and yellow were screened. The particles were prepared according to the method in section 3.4.1. The dyed particles were washed with ethanol (absolute), chloroform (100%) and 2 M NaCl solutions (1 ml) and recovered by centrifugation at 12470x g for 3 minutes. The supernatants from the different dyes were recovered and evaluated for dye leaching. Brilliant Yellow, Remazol Brilliant Blue R (RBBR) and Congo red were subsequently



chosen in this study as they demonstrated no dye leaching and were strongly associated with the particles.

*Table 1: Summary of the concentrations of dye used for dyeing particles.*

| Particle size ( $\mu\text{m}$ ) | Dye              | Concentration ( $\text{mg.ml}^{-1}$ ) |
|---------------------------------|------------------|---------------------------------------|
| 6                               | RBBR             | 8                                     |
|                                 | Congo Red        | 4                                     |
|                                 | Brilliant Yellow | 4                                     |
| 13 and 20                       | RBBR             | 4                                     |
|                                 | Congo Red        | 2                                     |
|                                 | Brilliant Yellow | 2                                     |

#### *3.4.2.1 Optimum wavelength determination*

The dye binding was calculated by difference i.e. dye solutions as prepared in section 2.4.1 were diluted and spectral analysis was performed using a Shimadzu UV-1650pc UV-VIS spectrophotometer using 1cm disposable UV-cuvette. The absorbance spectrum of each dye was recorded over the wavelength region of 300-700 nm. This was used to determine the absorbance maxima of each dye required for calculating the binding capacity of the particles in section 3.4.1.2.

#### *3.4.2.2 Dye binding capacity quantification*

The dye loading capacity of ReSyn™ particles was determined by quantifying the non-bound dye in the supernatant using absorbance analysis. The linear regression equation was solved to determine the unbound dye concentration of the different dyes. Fixed wavelengths 400 nm, 500 nm and 600 nm were used, corresponding to the absorbance maxima of RBBR, Congo Red and Brilliant Yellow respectively as obtained from the spectra shown in Figure 14. A dilution series of the different dyes were used to generate the standard curves (Appendix 1) used to evaluate dye binding.

## CHAPTER 4



## 4.1 Particle Preparation

Alterations in the emulsion parameters were investigated for the production of particles with different sizes. The type and concentration of surfactant and energy input were identified as suitable criteria for experimentation as these have been previously demonstrated to contribute to PSD in emulsion based particle preparation methods (Sajjadi *et al.*, 2003).

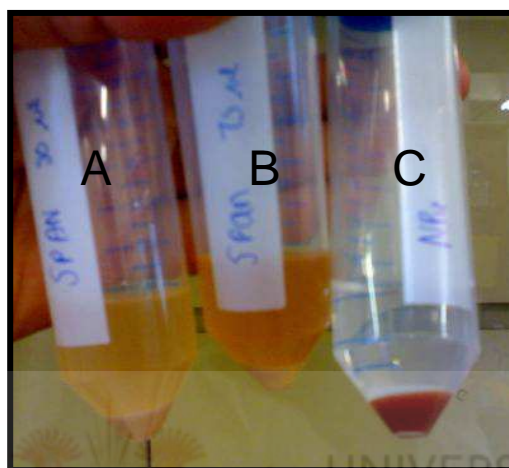


**Figure 12:** Image of the formed particles prior to the washing steps. Images A, B and C are 50, 75  $\mu$ l Span and 50  $\mu$ l NP4 particles respectively.

The polymer crosslinking reaction, which results in the formation of particles, occurs in the water phase of the emulsion. In the preparation method where Span20 (Figure 12) was used as a surfactant it appeared that some PEI may have dissolved in the oil phase rather than take part in the formation of the particles. This could have been due to the lipophilic property of Span detergents (Gullapalli *et al.*, 1999) which has a high affinity for the oil phase and may have dissolved some of the components in this phase.

The particles that could be recovered from the pellet after centrifugation were used for subsequent characterisation. The pellet was dried to determine the yield for the different preparation methods. The Span particles required a relatively high centrifugal force for pelleting. The parameters required for pelleting were 12470x g and extended up to 10 minutes to achieve a recoverable pellet during the washing steps.

## 4.2 Emulsion energy calculations

The following calculation present the first approximation towards determining the role energy plays in the preparation process. The system was treated as a solid as facilities for measuring parameters such as viscosity and friction were not available. The following function (A) was used to estimate the energy input in the emulsion based preparation process. Figure 13 outlines the model system used in the experiment. The following assumptions were made in calculating energy; complete homogenous mixing was achieved during the preparation steps, the fluid was considered incompressible and having uniform density, 100% of the energy in the system was incorporated in manufacturing the particles and the angular speed of all the particles in the fluid stayed constant throughout the vessel/ container. Up to date only the basic assumptions about the system and the type of energy involved were evaluated. Further experimentation and analysis must still be undertaken to fully recognise and understand the role that energy plays in this particular system.

$$E = 2 \left[ \frac{1}{2} m v^2 \right] t \int dr \int dz$$

E = kinetic energy of the system (Joules)

M = mass in kg of sample

v = velocity in meters.sec<sup>-1</sup> (mixing)

dr = radius in meters (vessel)

dz = distance in meters (sample movement during mixing)

t = Time of mixing (in seconds)

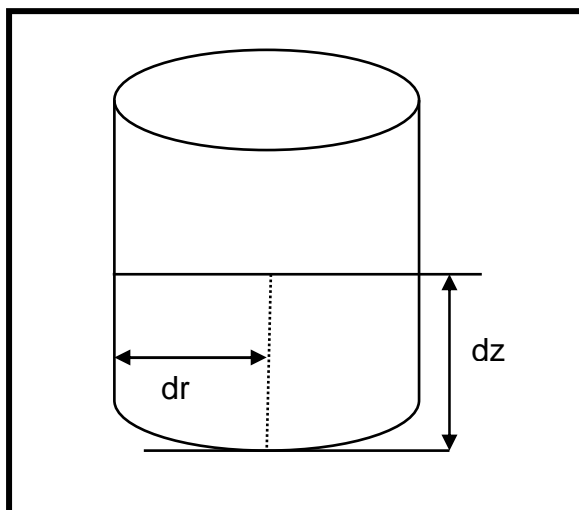


**Figure 13:** Representation of the preparation system (vessel). The vessel radius (dr) and the height (dz) is the assumed distance the sample travels within the vessel during the mixing process. These values in combination with the velocity and duration of mixing are used to calculate the energy used to achieve the emulsion in the system.

*Table 2:* Measurements of energy input for the different manufacturing procedures.

|                                                                                                                                                        |
|--------------------------------------------------------------------------------------------------------------------------------------------------------|
| <p>Particles manufactured using NP4</p> $2 \left\{ \frac{1}{2} (0.01769) (1.04)^2 (0.015) \right\} (0.042)(10)$ $= 1.20 \cdot 10^{-4} \text{ J}$       |
| <p>Particles manufactured using Span 20</p> $2 \left\{ \frac{1}{2} (0.01743) (0.2934)^2 (0.015) \right\} (0.025)(25)$ $= 2.36 \cdot 10^{-5} \text{ J}$ |

The manufacturing procedures used in this study were designed to achieve different sized particles based on changing reaction conditions. Energy input is a factor that could have a direct influence on the size of particles produced. (Table 2).

The Span particles were prepared using the same method and thus the same energy input, the resultant different particle sizes can be attributed to the concentration of surfactant. The NP4 particles were prepared using a higher

energy input i.e. 10 sec at 2500 rpm. Thus the smaller size may be attributed to the increased energy and the type of surfactant used.

The following factors were identified as contributing to the particle size of the preparations: surfactant concentration and type; energy input. These have previously been identified as mechanisms to control particle size (Lui *et al.*, 2005).

### 4.3 Dry weight determination

*Table 3:* Determination of particle yield by dry weight determination per starting raw material.

| Detergent type      | Particle Mass (mg) |          |          |         |
|---------------------|--------------------|----------|----------|---------|
|                     | Sample 1           | Sample 2 | Sample 3 | Average |
| NP4 (50 $\mu$ l)    | 20.4               | 18.88    | 19.00    | 19.4    |
| Span20 (50 $\mu$ l) | 15.6               | 15.2     | 15.4     | 15.4    |
| Span20 (75 $\mu$ l) | 6.4                | 6.00     | 6.2      | 6.2     |

The dry weight of each manufacturing process was evaluated to determine the yield from each emulsion preparation. The particles produced using NP4 as the detergent had the highest mass yield, while the use of the Span 20 (75  $\mu$ l) resulted in the lowest yield.

The dissolution of PEI in the oil phase (Figure 12) resulted in a decrease in available polymer for the formation of the particles. The particle mass as per preparation method is an important component of the process as it is the primary method of evaluating yield. This provides information on the reproducibility of the preparation process. Low recoveries in the case of Span could be associated with the loss of polymer to the oil phase as well as difficulties experienced during recovery.

### 4.4 Particle size distribution analysis

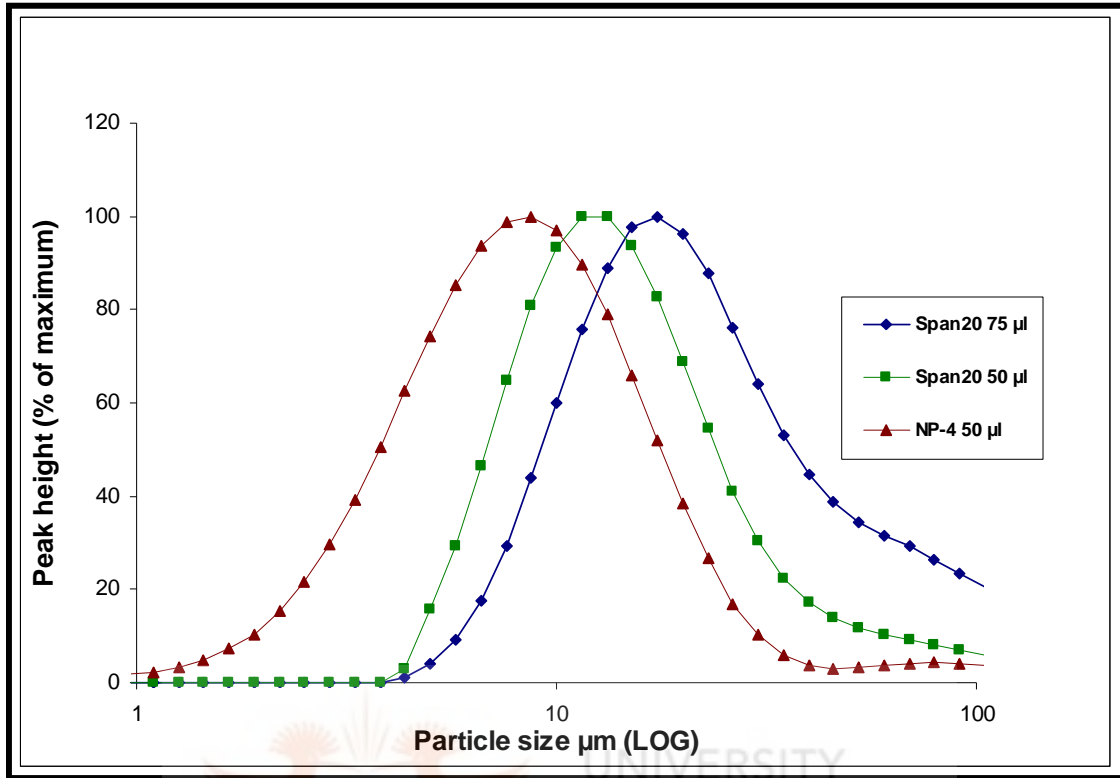


**Figure 14:** Particle size distribution (PSD) the particles produced using the different emulsion parameters. The red (—▲—) peak indicates the 6 μm particles followed by the green (—■—) peak for the 13 μm and the blue (—◆—) peak for the 20 μm particles.

**Table 4:** Laser diffraction statistics of the different sample populations.

|              | D(0.1) μm | D(0.5) μm | D(0.9) μm | D(3.2) μm | D(4.3) μm |
|--------------|-----------|-----------|-----------|-----------|-----------|
| Np4          | 3.163     | 7.740     | 18.954    | 5.990     | 14.246    |
| 50 μl Span20 | 6.762     | 12.951    | 37.494    | 11.993    | 23.698    |
| 75 μl Span20 | 9.087     | 19.519    | 73.986    | 17.284    | 32.380    |

Figure 14 displays the median (D (0.5)) value, indicating the average sizes obtained from analysis of the particles produced by the different preparation methods. The D (0.9) indicates that 10% of the particles have a greater size than 18.954 for 6 μm, 37.494 for 13 μm and 73.989 for 20 μm. The D (0.1) indicates that 10 % of the particles measured have sizes less than 3.163 μm, 6.762 for 13 μm and 9.087 for 20 μm. A three fold difference in the size

distribution is evident between the D (0.5) and D (0.9) for both the 13 and 20  $\mu\text{m}$  particles. The high D (0.9) values for the 13 and 20  $\mu\text{m}$  particle populations is an indication of a broad PSD, perhaps due to the presence of aggregates.

According to Moolman *et al.*, (2005) Span 20 which has a higher HLB factor should necessarily have resulted in smaller particles compared to the particles prepared using NP4 as a detergent. The current study has indicated results that are contrary to this study. Particles produced with Span20 as the surfactant were indeed larger than those produced using NP4 as the surfactant (Table 3). However, the nature of the liquids used in the preparation i.e. water and oil can influence particle size distribution as it may alter the way in which the detergent interacts with these liquids. The importance of the system conditions were investigated by Tai *et al.*, (2001) and the system as opposed to the surfactant alone contributes to the size and nature of the particle formed.

The concentration of the detergent used was another parameter that was investigated for the preparation of particles of distinct sizes. At different detergent concentrations the integrity of the emulsion is either reinforced or it is compromised. In a study by Ueyama *et al.*, (2000) the concentration of the surfactant was found to greatly influence the size of the particles produced. At low concentrations of  $20 \text{ g.L}^{-1}$  the average particle size was  $5 \mu\text{m}$  and concentration of  $80 \text{ g.L}^{-1}$  the particle size was reduced to  $0.5 \mu\text{m}$ .

Stringent control over microparticle size is an important requirement for size based applications. The applications of precision particles are size standards for flow cytometric analysis, cell estimation studies and fluid dynamic investigations. The current standard for variance in particle size standards is  $<3\%$ . The particles manufactured in this study are therefore not currently suitable as size standards. Further research in the formation of the emulsion will have to be conducted to improve the monodispersity of the particles.



## 4.5 Flow cytometric analysis

Analysis using flow cytometry was performed to determine the uniformity as well as the structural complexity of the particles produced using the different preparation methods. Figure 15 (A) 6  $\mu\text{m}$  particles, shows a population of particles that is compact in size and uniform. The side scatter is minimal indicating that the particles have similar spherical morphology.

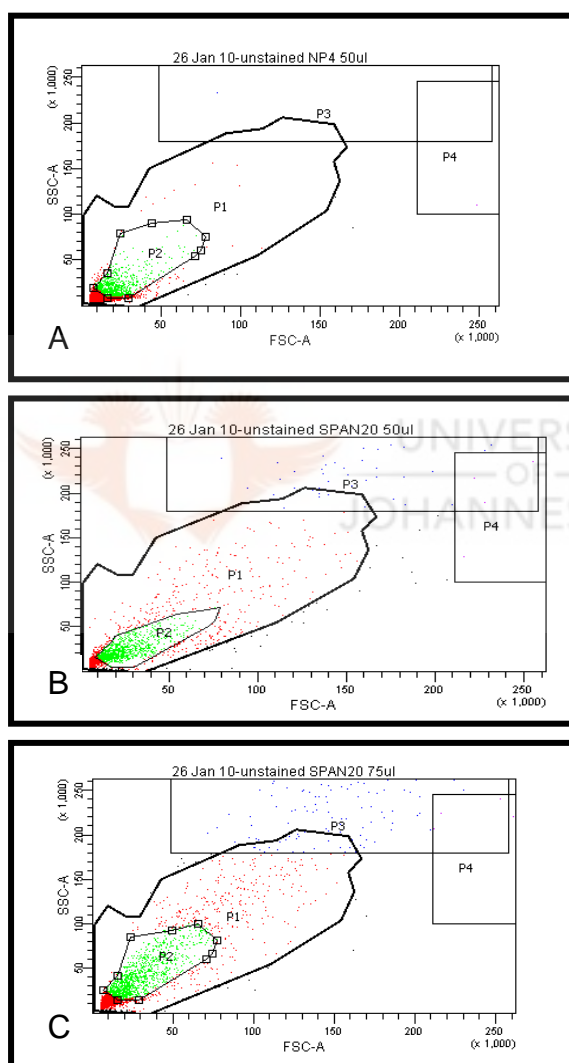
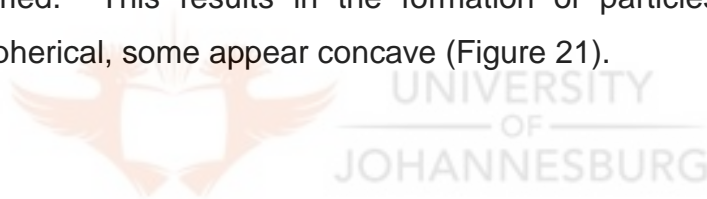


**Figure 15:** A, B and C are dot plots of the 6  $\mu\text{m}$ , 13  $\mu\text{m}$  and 20  $\mu\text{m}$  particle populations respectively. P1 represents the sample population, P2 was sorted for microscopic analysis as it was considered representative of the population, P3 represents the more complex particles in the population and P4 represents the large or aggregated particles in the sample.

The P1 region of the 13  $\mu\text{m}$  particles (Figure 15, B) indicates a bigger population size denoted by a shift to the right as compared to the P1 region of the 6  $\mu\text{m}$  particles. This is an indication of the difference in the size of particles produced. The complexity of the population may be due to aggregates formed as seen in the PSD analysis (Table 2) or the shape of the particles that are formed (Figure 21).

The 20  $\mu\text{m}$  sized particles have the highest population in the P3 region (Figure 15, C) indicating a high complexity. This is further supported by the presence of aggregates in the PSD for this particle preparation (Figure 14). It is further evident that the particle size is generally larger than the 6 and 13  $\mu\text{m}$  sample populations. The Span20 preparation method resulted in particles that are not completely spherical due to PEI being dissolved in the oil phase (Figure 12) rather than partaking in the crosslinking reaction, collapsing the particles formed. This results in the formation of particles that are not completely spherical, some appear concave (Figure 21).



#### 4.6 Morphological characterisation and analysis using microscopy

Microscopic analysis (Figure 16) confirms that in general the particles were of different sizes and supports the PSD data recorded (Table 3 and Figure 14). The images display smooth edged, spherical morphology of the particles as well as the similar distribution of sizes of the particle in each batch

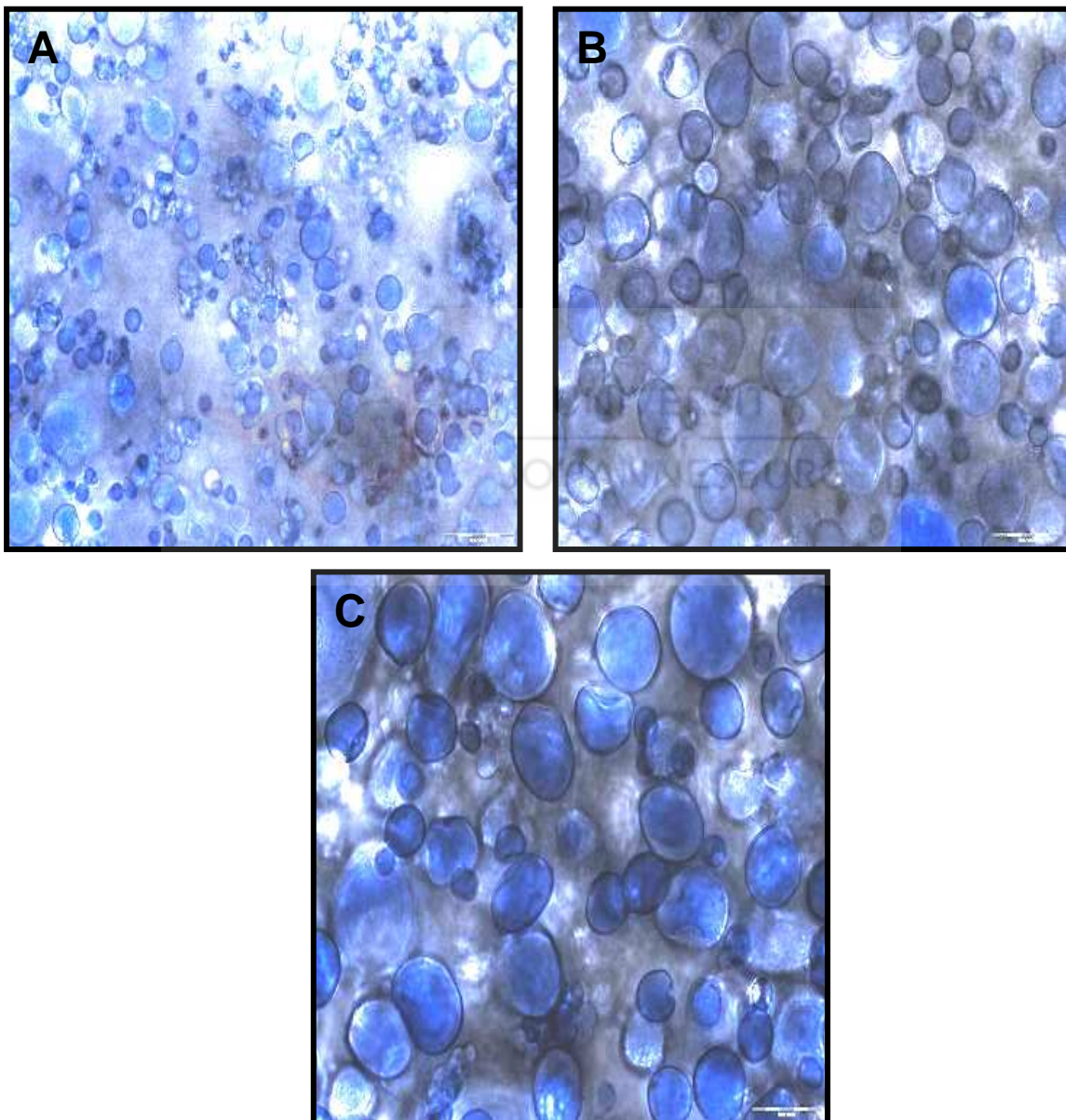


**Figure 16:** Microscopic images (P2 region of flow cytometry analysis) of the different particles produced and their size distribution. (A) Image of the 6  $\mu\text{m}$  sized particles (B) Image of the 13  $\mu\text{m}$  sized particles and (C) Image of the 20  $\mu\text{m}$  sized particles. (600x magnification).

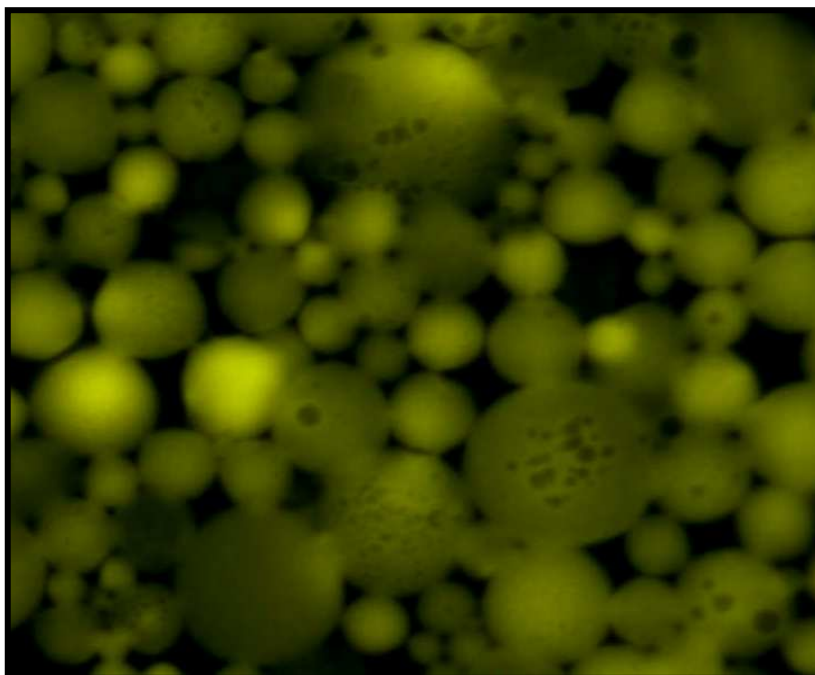


**Figure 17:** Light microscopy image of undyed ReSyn™ particles using a 100x oil immersion objective (1000x magnification).

#### 4.7 Particle density determination

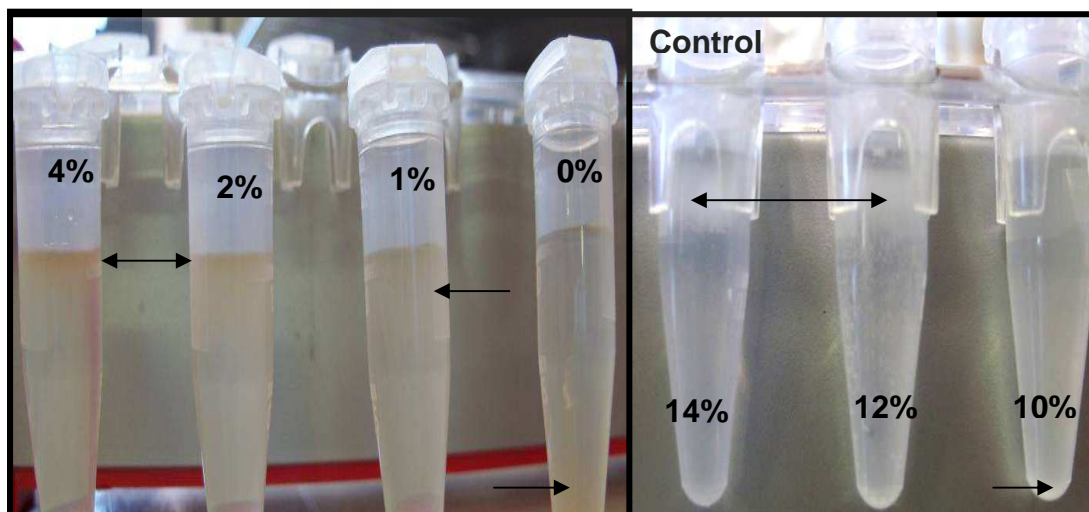


**Figure 18:** Particle density determination experimentation.

ReSyn™ particles have a lower density (Figure 18) compared to the commercially available polystyrene particles. The approximate density of ReSyn™ was found to be between  $1.0021 \text{ g.cm}^{-3}$  and  $1.0060 \text{ g.cm}^{-3}$ . The

density for 14% sucrose is  $1.0549 \text{ g.cm}^3$ . The control behaved as expected, with a density of  $1.05 \text{ g.cm}^{-3}$  they remained buoyant, indicating the validity of this technique for density determination.

Lateral flow assays require microparticles with good flow properties, and the density of the particulate system used influences this characteristic. The different particles available for this application range from  $0.4 \mu\text{m}$  to  $1 \mu\text{m}$  and are made from a variety of materials. Polystyrene particles of  $1.05 \text{ g.cm}^{-3}$  are used in diagnostic applications. The particle size is limited due to the hindrance to flow associated with larger particles. The ability to control the size and density, while maintaining other properties of interest, is a requirement for this application.

### **4.8 Dye binding capacity of the dyes**

#### **4.8.1 The absorbance spectra of RBBR, Congo Red and Brilliant Yellow**

The reactive dyes chosen for this application had to meet two criteria, (1) Dye must bind to the microparticles covalently (no leaching) and (2) the dyes must have distinct, non overlapping spectral wavelength maxima (Figure 19). These two requirements are important for applicability of microparticles as reagents in research and in multiplexing technologies.

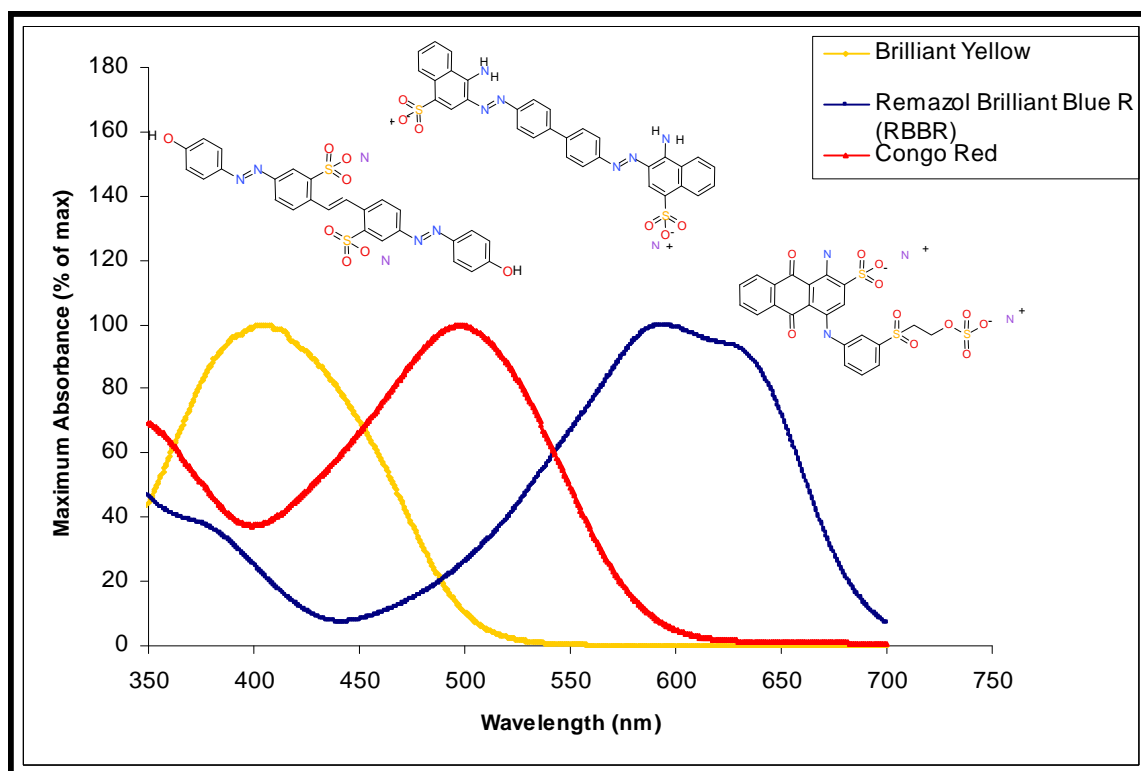


**Figure 19:** Absorbance spectra and chemical structures of the dyes used during experimentation. The blue, red and yellow curves represent RBBR, Congo Red and Brilliant Yellow respectively. The three dyes chosen have distinct spectral wavelength optima with limited overlap.

Multiplexing is a technique that requires the encoding of beads for identification of multiple analytes. The unique coding designated to each particle affords easy identification and detection (Figure 8; Nolan *et al.*, 2006). Beads can be coded in various ways e.g. beads of the same size are dyed using varying intensities of the one or more fluorophores or chromophores. Bead based arrays offer a more flexible choice and development of a new assay only requires the addition of a new bead with a different code i.e. a bead with a new identity (different Ab and colour). Decoding of beads in multiplexing assays can be achieved through the use of flow cytometers or optical reading platforms available (Birtwell *et al.*, 2010). The dyes RBBR, Congo Red and Brilliant Yellow were chosen after screening of a multitude of dyes (Appendix 2) as they met the two requirements of particles for this application, i.e. covalent attachment to the particles and distinct spectral wavelengths which define and give each bead in a population a unique

identity that can be easily detected. Wavelengths maxima for the different dyes were; RBBR 600nm, Congo Red, 500nm and Brilliant Yellow, 400nm

Covalent bonding of dyes with appropriate functionalities on microparticle is a great advantage as no leaching of the dye occurs. Leaching may indicate limitations for applications where particles are used after long term storage and stability of reagents is important e.g. rapid diagnostic tests.

#### 4.8.2 Percentage dye binding capacities of the different particle sizes

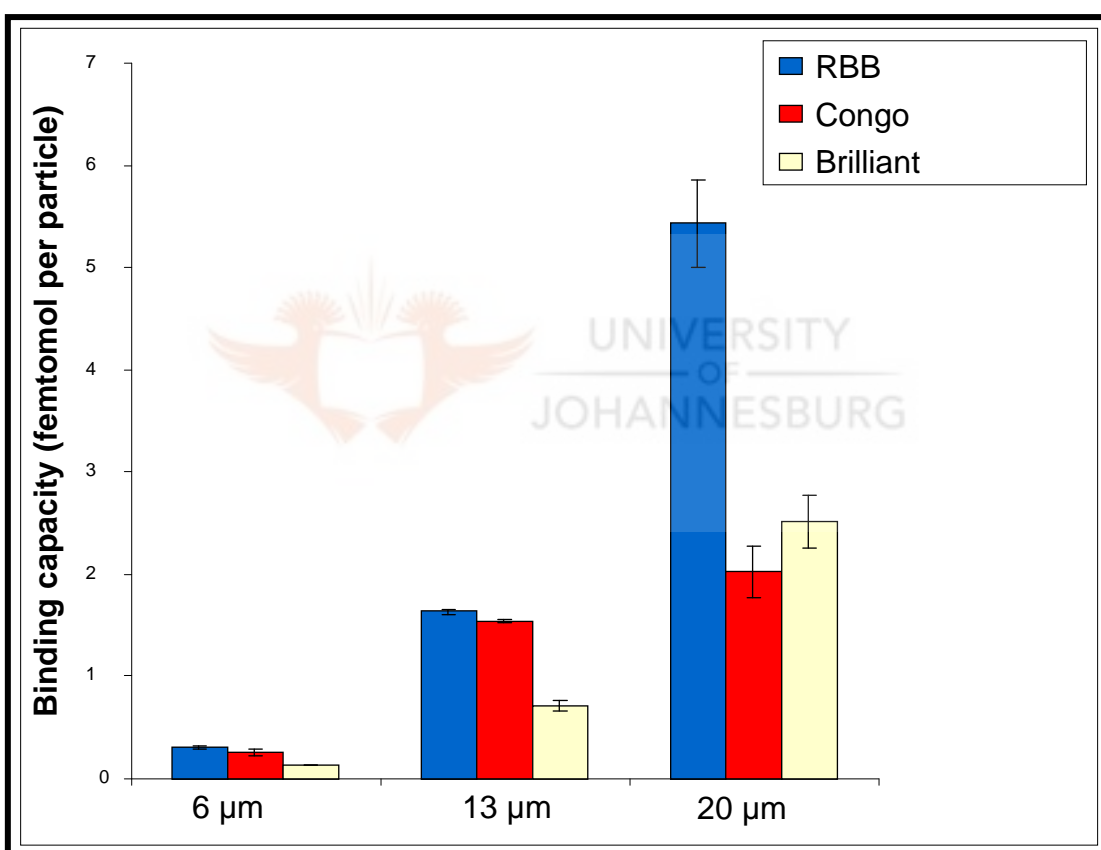


**Figure 20: Binding capacity (femtomol) of the different dyes based on the volume of individual particle sizes.**

Dye binding was achieved on all the particle sizes. The particles dyed with RBBR took up more dye (percentage) compared to the other dyes investigated in this study. Figure 20 shows the dye binding capacity achieved with the average particle sizes. The average volume of the different particle sizes was calculated (Appendix 3) to estimate the number of molecules

(moles) of dye bound to the particles. RBBR and Brilliant Yellow dyed particles show an exponential increase in binding capacity with an increase in particle size. A linear increase in binding capacity was observed with the Congo Red dyed particles with increase in particle size. An overall increase in dye binding capacity was observed with the different particle sizes from 6  $\mu\text{m}$  to 13  $\mu\text{m}$  to 20  $\mu\text{m}$  respectively and the dyes used.

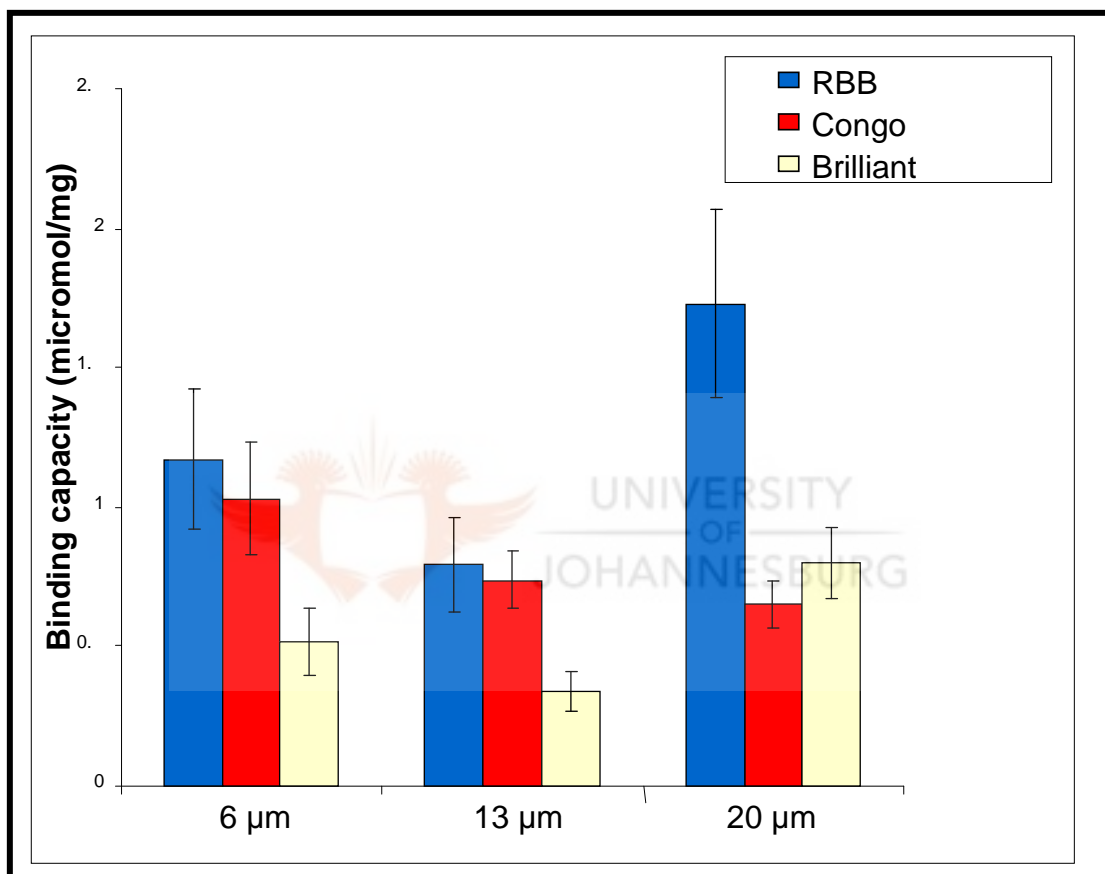


**Figure 21:** Dye binding (micromol) of the different dyes per mass of particles dyed. Comparison of the dye binding capacities of the different particle sizes with different dyes.

Particles (6  $\mu\text{m}$ ) dyed with RBBR and Congo Red (Figure 21) seem to have a similar binding capacity. The moles of dye bound per mg particle were  $1.17 \mu\text{mol.mg}^{-1}$  and  $1.03 \mu\text{mol.mg}^{-1}$  for RBBR and Congo Red respectively. However, Brilliant Yellow dyed particles showed a binding capacity of  $0.518 \mu\text{mol.mg}^{-1}$ , which is approximately 50% below that observed with RBBR and Congo Red. A similar binding pattern to that of the 6  $\mu\text{m}$  particles was



observed with the 13  $\mu\text{m}$  particles. RBBR and Congo Red bind similarly at 0.79 and 0.74  $\mu\text{mol}\cdot\text{mg}^{-1}$  respectively and Brilliant Yellow binds up to 50% less compared to RBBR and Congo Red at 0.339  $\mu\text{mol}\cdot\text{mg}^{-1}$ . A general decrease is observed in the binding capacity of the 13  $\mu\text{m}$  particles with all the dyes compared to that of 6  $\mu\text{m}$  particles. The 20  $\mu\text{m}$  RBBR and Brilliant Yellow dyed particles show an increase in dye binding capacity compared to the 6 and 13  $\mu\text{m}$  RBBR and Brilliant Yellow coloured particles. Binding capacity of RBBR and Brilliant Yellow was 1.73 and 0.81  $\mu\text{mol}\cdot\text{mg}^{-1}$  respectively. An approximate doubling in dye binding when compared to the RBBR coloured 13  $\mu\text{m}$  and 2.5 fold increase for the Brilliant Yellow particles. Congo Red dyed particles did not follow the same pattern observed with RBBR and Brilliant Yellow. A decrease in the amount of dye bound was observed. Congo Red binds 0.652  $\mu\text{mol}\cdot\text{mg}^{-1}$  a decrease from the 6 and 13  $\mu\text{m}$  Congo Red dyed particles.

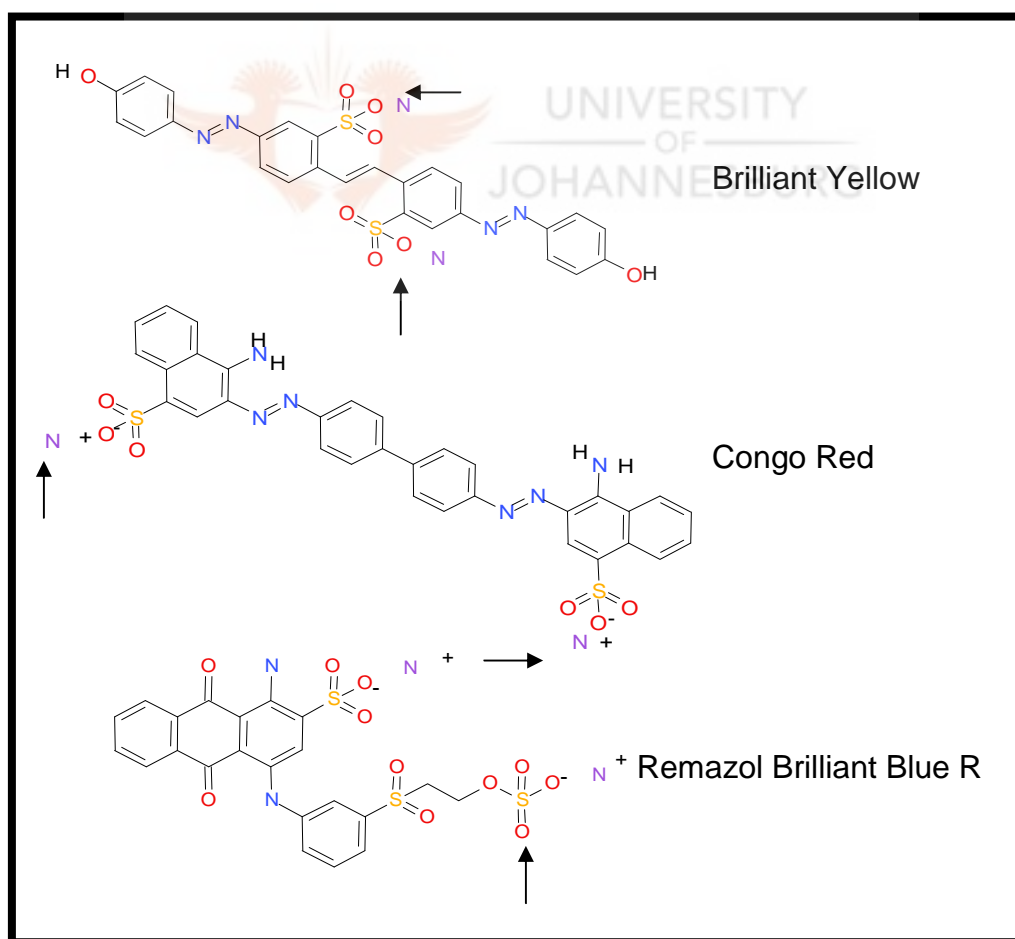


**Figure 22:** Dye molecule structures, arrows indicate position of functional groups for binding.

The 6 and 13  $\mu\text{m}$  particles show no difference in the binding capacity for RBBR and Congo Red. Congo Red contains terminal functional groups and RBBR contains a linker on one of the terminals making them more available for binding (Figure 22). However, there is a slight decrease in the amount of dye bound from the 6 to the 13 $\mu\text{m}$  particles indicating surface area limitations. Further investigation (Appendix 3) indicated that the decrease is not significant enough to be related to surface area phenomenon. A 4.6 fold decrease from 6  $\mu\text{m}$  to 13  $\mu\text{m}$  and 2.36 fold decrease from 13  $\mu\text{m}$  to 20  $\mu\text{m}$  indicates surface area related binding. The results show that a combination of surface area and penetration of dye may be occurring. Brilliant Yellow coloured particles bound up to 50% less in both the 6 and 13  $\mu\text{m}$  particles. The decrease in binding capacity may be attributed to steric hindrance. Brilliant Yellow contains functional groups that are positioned towards the middle of the molecule where access to binding sites can be obstructed (Figure 22). The low binding capacity may also be influenced by the duration of incubation during the binding process. The experiments for this study were timed and extensions in the incubation period may result in an increase in the binding of Brilliant Yellow.

The 20 micron particles showed an increase in binding capacity with both RBBR and Brilliant Yellow. This may be due to the availability of more binding sites on the particle. The 20  $\mu\text{m}$  particles may be more porous than the 6 and 13  $\mu\text{m}$  sized particles as a result of the preparation process where a significant amount of PEI was dissolved in the oil phase (Figure 12). The increased particle porosity could result in an increase in the number of available binding sites.

Congo red however deviates from the pattern observed with RBBR and Brilliant Yellow in that a decrease in binding is observed when compared to the other particle sizes. The increased porosity of the particle may be allowing the Congo Red molecules to act as crosslinking agents. The polymer strands may be positioned at distances that could allow both terminal groups of Congo Red to bind. This may increase the structural firmness of the particles as observed in Figure 23.

### 4.8.3 Microscopic analysis of coloured particles

Applications in imaging and flow cytometry require particles that can be discriminated easily against the background or in a mixture with other molecules and that are optically translucent (Sperling *et al.*, 2008).

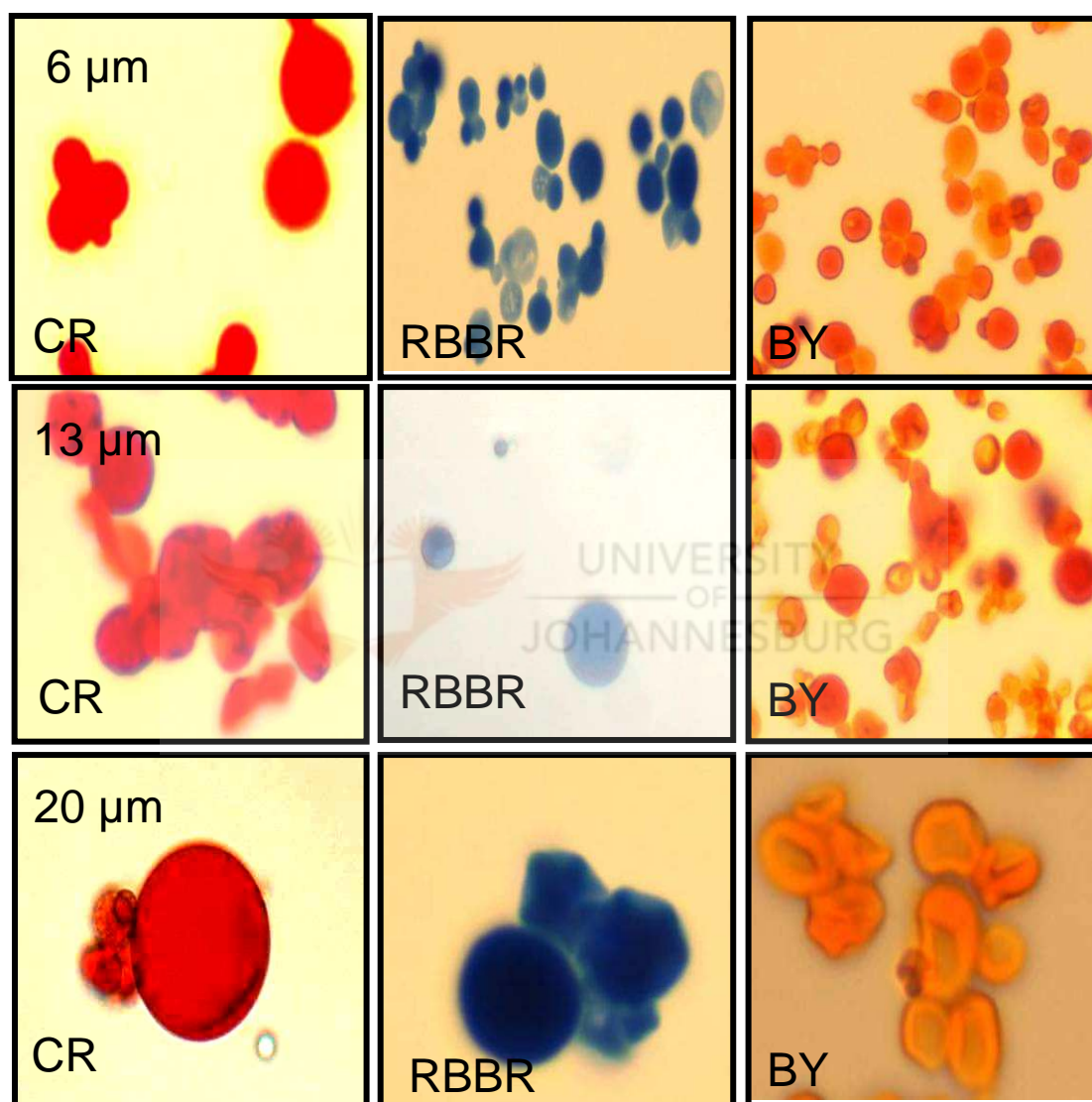


**Figure 23: Microscopic images of the different dyed particle preparations, showing the particles still retain their translucent property (1000x magnification).**

Images of the coloured particles were taken using a light microscope to investigate their visual properties. The morphology of the particles and the different colours of the dyes bound can be clearly visualised under the microscope (Figure 23). The dyes appear to bind throughout the volume of

the particles and not limited to the particle surface. The 20  $\mu\text{m}$  Brilliant Yellow dyed particles clearly show a collapsed structure and this may be attributed to the limited polymer available due to the dissolution of PEI in the oil phase (Figure 12). The 20  $\mu\text{m}$  Congo Red particles appear to be more structurally rigid compared to the 6 and 13  $\mu\text{m}$  sized particles. The particles do not appear to lose their translucent property even after dyeing.

### 4.9 Technology comparison

The high dye load can be attributed to the use of a loose polymer network instead of the typical solid particles that are routinely used in coloured microparticle applications discussed in Chapter 1. The high dye binding capacity of ReSyn™ makes them suitable for applications such as diagnostic detection agents where this feature can improve the sensitivity of the applications. Higher dye content can translate to improved visibility and easier detection (Posthuma-Trumpie *et al.*, 2009).

The ReSyn™ particles were compared to other commercially available coloured particles. These particles are marketed as having a standard dye content.

Table 5: A comparison of the particle technologies currently available for diagnostic applications.

| Brand                | Polymer     | Particle size ( $\mu\text{m}$ ) | Dye              | Dye load (% per weight) | Supplier          |
|----------------------|-------------|---------------------------------|------------------|-------------------------|-------------------|
| ReSyn™               | PEI         | 6                               | RBBR             | 45                      |                   |
|                      |             |                                 | Congo Red        | 39                      |                   |
|                      |             |                                 | Brilliant Yellow | 24                      |                   |
| Chromosphere         | Polystyrene | 0.47                            | All colours      | 14                      | Thermo Scientific |
| HiDye™               | PL-Latex    | 0.05-1                          | All colours      | 10                      | Varian Inc.       |
| Reagent microspheres | Polystyrene | 0.4                             | All colours      | 25                      | Brookhaven        |

Manufacturers of microparticles used in diagnostic test development provide particles that are small (submicron) in size for better flow properties as well as increased surface area. The particles also come in various colours for easy detection and visualisation which is important for detection. Commercially available diagnostic detection microparticles come in sizes ranging from 0.05-1  $\mu\text{m}$  and dye loading from 10-25% (Table 5). ReSyn™ particles currently exceed what is commercially available in terms of the amount of dye that can be loaded onto the particle. Properties such as size distribution and uniformity still require optimisation to be suitable for application as diagnostic detection agents. The 6  $\mu\text{m}$  RBBR coloured microspheres can load up to 45% dye per particle which is better by a factor of 1.8 compared to other particles.

Table 6: A comparison of the coloured microspheres used in applications other than diagnostics.

| Brand                     | Polymer                    | Particle size (µm) | Dye              | Dye load (%per weight) | Supplier        |
|---------------------------|----------------------------|--------------------|------------------|------------------------|-----------------|
| ReSyn™                    | PEI                        | 6                  | RBBR             | 45                     | N/A             |
|                           |                            |                    | Congo Red        | 39                     |                 |
|                           |                            |                    | Brilliant Yellow | 24                     |                 |
| ReSyn™                    | PEI                        | 13                 | RBBR             | 35                     | N/A             |
|                           |                            |                    | Congo Red        | 31                     |                 |
|                           |                            |                    | Brilliant Yellow | 17                     |                 |
| ReSyn™                    | PEI                        | 20                 | RBBR             | 54                     | N/A             |
|                           |                            |                    | Congo Red        | 28                     |                 |
|                           |                            |                    | Brilliant Yellow | 33                     |                 |
| ChromoSphere              | Polystyrene divinylbenzene | 49                 | All colours      | 5                      | Duke-Scientific |
| Polyethylene microspheres | Polyethylene               | 20-27              | Black            | 20                     | Cospheric       |
|                           |                            |                    | Blue             | 5                      |                 |

These polymer particles are applied in the testing of filtration media and systems, sedimentation processes, pharmaceutical, fillers, carriers, or active ingredients in paints, coatings, cosmetics and imaging. The characteristic requirements for these applications are different to those in diagnostics. For application in imaging the high contrast and visibility is required to distinguish the particles from the background. The size of the microparticles is also

negligible depending on the end application. Commercially available microparticles range between 1 and 1000  $\mu\text{m}$ . Comparison with current technology concentrated on particles with sizes ranging from 20-27  $\mu\text{m}$  with a dye loading capacity of between 5-20% (Gobrogge, 2010) as a direct comparison can be done with ReSyn™. ChromoSpheres from Duke scientific are 49  $\mu\text{m}$  in size with a dye binding capacity of 5% for all colours (Dukescientific.,2009 ). The high dye binding capacity indicates that ReSyn™ may have application in these technologies; more specifically the high dye binding capacity may assist in improving the sensitivity of these various applications. The highest dye load achieved was 54% (Table 6) using RBBR as the dye. This is 2.7 fold better than existing microparticle technologies.



## CHAPTER 5



## CONCLUSIONS



The study identified three parameters that are important for a variety of microparticle applications. These are particle size, particle size distribution and optical properties.

These parameters were investigated to elucidate the potential for application of proprietary particles according to WO2009057049 as detection agents. Emulsion parameters were controlled by changing reaction conditions, including detergent type and concentration, which yielded average particle sizes of 6, 13 and 20  $\mu\text{m}$  in diameter. Of further interest was the effect of energy to control particle size. However, this appeared to be a less important criterion.

The PSD results of the various preparations showed the populations were polydisperse. The wide PSD could be a result of factors such as non-uniform energy dispersion. Investigation of alternate energy delivery systems for the preparation of microparticles could possibly result in the production of particles with a narrower particle size distribution. Alternate methods for particle preparation, such as the use of microfluidic technologies, or the use of alternate energy sources such as sound, may improve particle uniformity. A narrow particle size distribution is desirable as it can influence reproducibility in applications such as flow cytometry. The particle uniformity is at present not optimal for application as a diagnostic detection agent. Further studies on controlling preparation parameters to achieve a more uniform and narrow PSD will be undertaken for ReSyn™ to expand the potential applications.

The particles bound high quantities of dye in comparison to alternate bead based technologies. The combination of particle size and dye structure was found to influence binding capacity. ReSyn™ particles achieved a maximum dye binding of 54% of the final dry weight. This is more than double that of the nearest alternate technology. Dyeing the particles increased their visibility under the microscope. The coloured microspheres were chemically stable and exhibited no dye leaching under stringent elution conditions. This is indicative of the stability of the particles, which is important for applications where reagent storage for extended periods of time is required e.g. point-of-

care diagnostic devices. Further studies such as storage stability are required for commercial use.

Visual and optical properties of the particles are important for applications such as flow cytometric and diagnostic detection agents. Improved dye loads may improve the visibility of particles, potentially resulting in improved ease of detectability. The translucent nature of the particles is a property that is useful in flow cytometric applications, ReSyn™ particles retain their optical translucency, even after dyeing. The ability to detect analytes at very low concentrations can greatly improve the performance of immunoassays. The high dye binding achieved with ReSyn™ indicates that the particles are potentially suitable for applications where improvements in sensitivity are required, without compromising on other properties that are already established, such as size and particle chemistry. Application of ReSyn™ as detection agents in diagnostics and multiplex assays can be explored further. The ability to attach different chromophores to confer unique codes needs to be evaluated for the application of these particles in flow cytometry.

In conclusion, the novel proprietary polymer particle technology ReSyn™ has been evaluated as a promising particulate system for application as a detection agent. The high dye binding capacity, stability, and ability to control emulsion parameters for the preparation of particles of different sizes, indicates it is potentially suitable for the development of a variety of applications. Bead based assays including rapid diagnostic tests and multiplex assays can benefit from particle systems with excellent visual properties, as it can possibly enhance the performance and efficiency of potential applications.



Agasti, S., Rana, S., Park, M., Kim, C., You, C. and Rotello, V. (2010) Nanoparticles for detection and diagnosis, *Advanced Drug Delivery Reviews*, vol. 62, no.3, pp.316-328

Andersson, H. and van den Berg, A. (2003) Microfluidic devices for cellomics: a review, *Sensors and Actuators B: Chemical*, vol. 92, no. 3, pp. 315-325.

Andreotti, P., Ludwig, G., Peruski, A., Tuite, J., Morse, S. and Peruski, Jr. L. (2003) Immunoassay of infectious agents, *BioTechniques*, vol 35, pp 850-859

Antonietti, M., Lohmann, S. and Van Niel, C. (1992) Polymerisation in Microemulsion. 2. Surface Control and Functionalization of Microparticles, *Macromolecules*, vol. 25, pp. 1139-1143

Bange, A., Halsall, B. and Heineman, W. (2005) Microfluidic immunosensor systems, *Biosensors and Bioelectronics*, vol. 20, pp. 2488-2503

Bangs, L. and Meza, M. (1994) Microspheres, part 1: selection, cleaning and characterisation

Bangs Labs, Technical note 301, available online, ([www.bangslabs.com](http://www.bangslabs.com) accessed 25 January 2010)

Bangs Labs, Technical note 303, available online, ([www.bangslabs.com](http://www.bangslabs.com) accessed 25 January 2010)

Baptista, P., Pereira, E., Eaton, P., Doria, G., Miranda, A., Gomes, I., Quaresma, P. and Franco, R. (2008) Gold nanoparticles for the development of clinical diagnosis methods, *Analytical Bioanalytical Chemistry*, vol. 391, pp. 943-950

Beebe, D., Mensing, G. and Walker, G. (2002) Physics and Application of Microfluidics in Biology, *Annual Review of Biomedical Engineering*, vol. 4, no. 1, pp. 261-286.

- Bell, D., Wongsrichanalai, C. and Barnwell, J. (2006) Evaluation of Rapid Diagnostic Tests: Malaria, *Nature Reviews Microbiology*, vol 4, pp. 682-695
- BD Biosciences (2000) Introduction to Flow Cytometry, Manual Part Number 11-11032-01
- Biro, E., Nemeth, A., Feczko, T., J., Sisak, C., and Gyenis, J. (2008) Preparation of chitosan particles suitable for enzyme immobilization, *Journal of Biochemical and Biophysical Methods*, vol. 70, no. 6, pp. 1240-1246
- Biro, E., Nemeth, A., Feczko, T., Tóth, J., Sisak, C., and Gyenis, J. (2009) Three-step experimental design to determine the effect of process parameters on the size of chitosan microspheres, *Chemical Engineering and Processing: Process Intensification*, vol. 48, no. 3, pp. 771-779
- Birtwell, S. and Morgan, H. (2010) Microparticle encoding technologies for high-throughput multiplexed suspension assays, Proceedings of the 3rd International Conference on the Development of BME in Vietnam, 11-14th Jan 2010
- Bonenberger, J. and Doumanas, M. (2006) Overcoming sensitivity limitations of lateral-flow immunoassays with a novel labeling technique, IVD Technology available online, ([www.ivdtechnology.com/article/overcoming-sensitivity-limitations-lateral-flow-immunoassays-novel-labeling-technique](http://www.ivdtechnology.com/article/overcoming-sensitivity-limitations-lateral-flow-immunoassays-novel-labeling-technique) accessed 15 February 2010)
- Brady, D., Jordaan, J. (2009) Advances in enzyme immobilisation, *Biotechnology Letters*, vol. 31, pp. 1639-1650
- Brookhaven, available online, ([www.brookhaven.com](http://www.brookhaven.com) accessed 25 January 2010).

- Brown, M. and Wittwer, C. (2000) Flow Cytometry: Principles and Clinical Applications in Hematology, *Clinical Chemistry*, vol. 46 no.8(B), pp. 1221–1229
- Çakmak, S., Gümüşderelioğlu, M. and Denizli, A. (2009) Biofunctionalization of magnetic poly(glycidyl methacrylate) microspheres with protein A: Characterization and cellular interactions, *Reactive & Functional Polymers*, vol. 69, pp. 586–593
- Camilla, C., Mély, L., Magnan, A., Casano, B., Prato, S., Debono, S., Montero, F., Defoort, J Martin, M. and Fert, V. (2001) Flow Cytometric Microsphere-Based Immunoassay: Analysis of Secreted Cytokines in Whole-Blood Samples from Asthmatics, *Clinical and Diagnostic Laboratory Immunology*, vol. 8 no.4, pp. 776-784
- Campbell, M. (1991) Biochemistry, international Edition, Saunders College Publishing, Chapter 8, pp 150-156
- Carville, D. (2007) Microparticle technology in clinical diagnostics recent advances in detection sensitivity and POC platform utility promise faster, more accurate patient triage, available online, ([www.medicaldevicelink.com](http://www.medicaldevicelink.com) accessed 15 February 2010)
- Chard, T. (1992) Pregnancy tests: a review, *European Society of Human Reproduction and Embryology* , vol. 7, no. 5, pp. 701-710
- Chithrani, D., Ghazani, A. and Chan, W. (2006) Determining the size and shape dependence of gold nanoparticles uptake into mammalian cell, *Nano Letters*, vol. 6, no. 4, pp. 662-668
- Choi, D., Lee, S., Oh, Y., Bae, B., Lee, S., Kim, S., Shin, Y. and Kim, M. (2010) A dual gold nanoparticle conjugate-based lateral flow assay (LFA) method for the analysis of troponin I, *Biosensors and Bioelectronics*, vol.25, no. 8, pp. 1999-2002

- Chu, X., Fu, X., Chen, K., Shen, G. and Yu, Q. (2005) An electrochemical stripping of metalloimmunoassay based on silver enhanced gold nanoparticles label, *Biosensors and Bioelectronics*, vol. 20, pp. 1805-1812
- Compton, M., Lapp, S. and Pedemonte, R. (2002) Generation of multicoloured, prestained molecular weight markers for gel electrophoresis, *Electrophoresis*, vol. 23, pp. 3262-3265
- Derveaux, S., Stubbe, B., Braeckmans, K., Roelant, C., Sato, K., Demeester, J. and De Smedt, S (2008) Synergism between particle-based multiplexing and microfluidics technologies may bring diagnostics closer to the patient, *Analytical Bioanalytical Chemistry*, vol. 391, pp. 2453–2467
- Dendukuri, D. and Doyle, P. (2009) The Synthesis and Assembly of Polymeric Microparticles Using Microfluidics, *Advanced Materials*, vol. 21, pp. 1–16
- Dini, E., Alexandridou, S. and Kiparissides, C. (2003) Synthesis and characterization of cross-linked chitosan microspheres for drug delivery applications, *Journal of microencapsulating*, vol. 20 no. 3, pp. 375–385
- Duke Scientific, available online, ([www.dukescientific.com](http://www.dukescientific.com) accessed 20 January 2010)
- Fenniri, H. and Alvarez-Puebla, R. (2007) High-throughput screening flows along, *Nature Chemical Biology*, vol. 3 no. 5, pp.247-249
- Franse, M., Blankwater, I. and Valentine M. (2008), WO20080227220
- Fu, W., Shenoy, D., Li, J., Crasto, C., Jones, G., Dimarzio, C., Sridhar, S. and Amiji, M. (2005) Biomedical Applications of Gold Nanoparticles Functionalized Using Hetero-Bifunctional Poly(ethylene glycol) Spacer, *Materials Research Society*, vol. 845, pp. AA5.4.1- AA5.4.6

- Gañán-Calvo, A., Martín-Banderas, L., González-Prieto, R., Rodríguez-Gil, A., Berdúm-Álvarez, T., Cebolla, A., Chávez, S. and Flores-Mosquera, M. (2006) Straightforward production of encoded microbeads by Flow Focusing: Potential applications for biomolecule detection, *International Journal of Pharmaceutics*, vol. 324, pp 19-26
- Gobrogge, B. (2010) Properties of coloured microspheres, Personal communication, 15 January 2010, email- [brian@cospheric.com](mailto:brian@cospheric.com), tel. +1 805 687 3747
- Gosh, P., Han, G., De, M., Kim, C. and Rotello, V. (2008) Gold nanoparticles in delivery applications, *Advanced Drug Delivery Reviews*, vol. 60, no. 11, pp. 1307-1315
- González, L., Villa de, A., Montes de, C. and Gelbard, G. (2005) Immobilisation of methytrioxorhenium onto tertiary amine and pyridine N-oxide resins, *Reactive and Functional Polymers*, vol. 65, pp. 169-181
- Gullapalli, R. and Sheth, B. (1999) Influence of an optimized non-ionic emulsifier blend on properties of oil-in-water emulsions, *European Journal of Pharmaceutics and Biopharmaceutics*, vol. 48, pp. 233-238
- Gurkov, T., Horozov, T., Ivanov, J. and Borwankar, R. (1994) Composition of mixed adsorption layers of non-ionic surfactants on oil/water interfaces, *Colloids and Surfaces A: Physicochemical and Engineering Aspects*, vol. 87, pp. 81-92
- Holmes, D., She, J., Roach, P. and Morgan, H. (2007) Bead-based immunoassays using a micro-chip flow cytometer, *Lab Chip, The Royal Society of Chemistry*, vol. 7, pp. 1048-1056
- Hicks, J. *Comprehensive Chemistry, SI Edition, Revised 2nd edition*, The MACMILLAN press Ltd, (1971), pp.264



- Jang, J. and Lee, K. (2002) Facile fabrication of hollow polystyrene nanocapsules by microemulsion polymerization, *The Royal Society of Chemistry, Chemistry Communication*, pp. 1098–1099
- Joos, T., Stoll, D. and Templin, M. (2002) Miniaturised multiplexed immunoassays, *Current Opinion in Chemical Biology*, vol, 1, no. 1, pp. 76-80
- Jordaan, J., Simpson, C., Brady, D., Gardiner, N. S. & Gerber, I. B. (2009), WO2009057049
- Kah, J., Olivo, M., Lee, C. and Sheppard, C. (2008) Molecular contrast of EGFR expression using gold nanoparticles as a reflectance-based imaging probe, *Molecular and Cellular Probes*, vol, 22, no. 1, pp. 14-23
- Kawaguchi, H. (2000) Functional polymer microspheres, *Progress in Polymer Science*, vol. 25, pp. 1171-1210
- Kellar, K. and Iannone, M. (2002) Multiplexed microsphere- based flow cytometric assays, *Experimental Hematology*, vol. 30, pp. 1227-1237
- Kuntaegowdanahalli, S., Bhagat, A, Kumar, G. and Papautsky, I. (2009) Inertial microfluidics for continuous particle separation in spiral microchannels, *Lab Chip, The Royal Society of Chemistry*, vol. 9, pp. 2973-2980
- Lee, Y., Oh, C., Koo, S. and Oh, S. (2005) New approach for the control of size and surface characteristics of mesoporous silica particles by using mixed surfactants in W/O emulsion, *Microporous and Mesoporous Materials*, vol. 86, pp. 134–144
- Lei, C., Shin, Y., Liu, J. and Ackerman, E. (2002) Entrapping Enzyme in a Functionalized Nanoporous Support, *Journal of the American Chemical Society*, vol. 124, pp. 11242-11243

- Ling, J., Li, Y. and Huang, C. (2009) Visual sandwich immunoassay system on the basis of Plasmon resonance scattering signals of silver Nanoparticles, *Analytical Chemistry*, vol. 81, pp. 1707–1714
- Liu, E. and McGrath, K. (2005) Emulsion microstructure and energy input, roles in emulsion stability, *Colloids and Surfaces A: Physicochemical and Engineering Aspects*, vol. 262, pp. 101-112
- Liu, Y., Zhang, D., Alocilja, E. and Chakrabartty, S. (2010) Biomolecules Detection Using a Silver-Enhanced Gold Nanoparticle-Based Biochip, *Nanoscale Research Letters*, DOI 10.1007/s11671-010-9542-0
- Martín-Banderas, L., Rodríguez-Gil Á., Cebolla, A., Chávez, S., Berdún-Álvarez, T., Fernandez Garcia, J., Flores-Mosquera, M. and Gañán-Calvo, A. (2006) Towards High-Throughput Production of Uniformly Encoded Microparticles, *Advanced Materials*, vol. 18, no. 5, pp. 559-564
- Mercolino, J., Hasskamp, J. and McFarland, E. (1994), 5369036
- Mitragotri, S. and Lahann, J. (2008) Physical approaches to biomaterial design, *Nature Materials*, vol. 8, pp. 15-23
- Moolman, F., Brady, D., Sewlall, A., Rolfes, H. and Jordaan, J. (2005), WO200508561
- Müller, R., Rühl, D., Lück, M. and Paulke, B. (1997) Influence of Fluorescent Labelling of Polystyrene Particles on Phagocytic Uptake, Surface Hydrophobicity, and Plasma protein Adsorption, *Pharmaceutical Research*, vol. 14 no. 1, pp. 18-24

- Murakami, Y., Endo, T., Yamamura, S., Nagatani, N., Takamura, Y. and Tamiya, E. (2004) On-chip micro-flow polystyrene bead-based immunoassay for quantitative detection of tactrolimus (FK506), *Analytical Biochemistry*, vol. 334, pp. 111-116
- Newman, G. and Jasani, B., Silver development in microscopy and bioanalysis: past and present, *The Journal of Pathology*, vol. 186, no. 2, pp. 119-125
- Nolan, J. and Mandy, F. (2006) Multiplexed and Microparticle-based Analyses: Quantitative Tools for the Large-Scale Analysis of Biological Systems, *Cytometry A*, vol. 69, no. 5, pp. 318–325.
- Park, S., Kim, K. and Kim, H. (2002) Preparation of silica nanoparticles: determination of the optimal synthesis conditions for small and uniform particles *Colloids and Surfaces A: Physicochemical Engineering Aspects*, vol. 197, pp. 7–17
- Penn, S., He, L. and Natan, M. (2003) Nanoparticles for bioanalysis, *Current Opinion Chemical Biology*, vol. 7, pp. 609–615
- Pichot, C. (2004) Surface-functionalized latexes for biotechnological applications, *Current Opinion in Colloid & Interface Science*, vol. 9, pp. 213–221
- Posthuma-Trumpie, G., Korf, J. and van Amerongen A, (2009) Lateral flow (immuno) assay: its strengths, weaknesses, opportunities and threats. A literature survey, *Analytical and Bioanalytical Chemistry*, vol. 393, pp. 569-582
- Rembaum, A., Yen, S., Cheong, E., Wallace, S., Molday, R., Gordon, I. and Dreyer, W. (1976) Functional Polymeric Microspheres Based on 2-Hydroxyethyl Methacrylate for Immunochemical Studies<sup>1</sup>, *Macromolecules*, vol. 9, No. 2, pp. 328-336

- Risbud, M., Hardikar, A., Bhat, S. and Bhonde, R. (2000) pH-sensitive freeze-dried chitosan–polyvinyl pyrrolidone hydrogels as controlled release system for antibiotic delivery, *Journal of Controlled Release*, vol. 68, no 1, pp. 23-30
- Rong-Hwa, S., Shiao-Shek, T., Der-Jiang, C. and Yao-Wen, H. (2010) Gold nanoparticle-based lateral flow assay for detection of staphylococcal enterotoxin B, *Food Chemistry*, vol. 118, pp. 462-466
- Rosi, N. and Mirkin, C. (2005) Nanostructures in Biodiagnostics, *Chemical Reviews*, vol. 105, no. 4, pp. 1547-1567
- Rundström, G., Jonsson, A., Mårtensson, O., Mendel-Hartvig, I. and Venge, P. (2007) Lateral Flow Immunoassay Using Europium (III) Chelate Microparticles and Time-Resolved Fluorescence for Eosinophils and Neutrophils in Whole Blood, *Clinical Chemistry*, vol. 53 no.2, pp.342–348
- Sajjadi, S., Zerfa, M. and Brooks, B. (2003) Phase inversion in p-xylene/water emulsions with the non-ionic surfactant pair sorbitan monolaurate/polyoxyethylene sorbitan monolaurate (Span 20/Tween 20) *Colloids and Surfaces A: Physicochemical Engineering Aspects*, vol. 218, pp. 241- 254
- Salager, J., Perez-Sanchez, M. and Garcia, Y. (1996) Physicochemical parameters influencing the emulsion drop size, *Colloid Polymer Science*, vol. 274, pp. 81-84
- Sanvicens, N. and Marco, M. (2008) Multifunctional nanoparticles properties and prospects for their use in human medicine, *Trends in Biotechnology*, vol. 26, no. 8, pp. 425-433
- Sato, K., Tokeshi, M., Odake, T., Kimura, H., Ooi, T., Nakao, M. and Kitamori, T. (2000) Intergration of an immunosorbent Assay System: Analysis of Secretory Human Immunoglobulin A on Polystyrene Beads in a Microchip, *Analytical Chemistry*, vol. 72, pp. 1144-1147

- Schwartz, A., Marti, G., Poon, R., Gratama, J. and Fernandez-Repollet, E. (1998) Standardizing Flow Cytometry: A Classification System of Fluorescence Standards Used for Flow Cytometry, *Cytometry* 33:106–114
- Seydack, M. (2005) Nanoparticle labels in immunosensing using optical detection methods, *Biosensors and Bioelectronics*, vol. 20, pp. 2454–2469
- Shyu, R., Shyu, H., Liu, H. and Tang, S. (2002) Colloidal gold-based immunochromatographic assay for detection of ricin, *Toxicom*, vol. 40, pp. 255-258
- Sivagnanam, V., Song, B., Vandevyver, C. and Gijs, M. (2009) On-Chip Immunoassay Using Electrostatic Assembly of Streptavidin-Coated Bead Micropatterns, *Analytical Chemistry*, vol. 81, pp. 6509-6515
- Sperling, R. Gil, P., Zhang, F., Zanella, M. and Parak, W. (2008) Biological applications of gold nanoparticles, *Chemical Society Reviews*, vol. 37, pp. 1896 – 1908
- Spherotech (2009) Measuring Absolute Cell Count using SPHERO™ Accucount Fluorescent Particles, available online, ([www.spherotech.com](http://www.spherotech.com) accessed 12 February 2010)
- Stejskal, J., Sulimenko, T., Prokesi, J. and Sapurina, I. (2000) Polyaniline dispersions 10. Coloured microparticles of variable density prepared using stabilizer mixtures, *Colloid Polymer Science*, vol. 278, pp. 654-658
- Stirhoff, J., Lazarides, A., Mucic, R., Mirkin, C., Letsinger, R. and Schatz, G. (2000) What Controls the Optical Properties of DNA-Linked Gold Nanoparticle Assemblies? *Journal of the American Chemical Society*, vol. 122, no. 19, pp. 4640-4650
- Tai, C., Lee, M. and Wu, Y. (2001) Control of zirconia particle size by using two-emulsion precipitation technique, *Chemical Engineering Science*, vol. 56, pp. 2389-2398

Takahashi, T., Ogata, S., Nishizawa, M. and Matsue, T. (2003) A valveless switch for microparticle sorting with laminar flow streams and electrophoresis perpendicular to the direction of fluid stream, *Electrochemistry Communications*, vol. 5, pp. 175-177

Thermo Scientific, available online, ([www.thermoscientific.com](http://www.thermoscientific.com), accessed 20 January 2010)

Thiele, L., Merkle, H, and Walter, E. (2003) Phagocytosis and Phagosomal Fate of Surface-Modified Microparticles in Dendritic Cells and Macrophages, *Pharmaceutical Research*, vol. 20, No. 2, pp.

Tozzoli, R. (2007) Recent advances in diagnostic technologies and their impact in autoimmune diseases, *Autoimmunity Reviews*, vol. 6, pp. 334–340

Uchiyama, K., Nakajima, H. and Hobo, T. (2004) Detection methods for microchip separations, *Analytical Bioanalytical Chemistry*, vol. 379, pp. 375–382

Ueyama, R., Harada, M., Ueyama, T., Yamamoto, T., Shiosaki, T., Kuribayashi, K., Koumoto, K. and Son Seo, W. (2000) Preparation of BaTiO<sub>3</sub> ultrafine particles by micro-emulsion charring method, *Journal of Materials Science: Materials in Electronics*, vol. 11, pp. 139-143

van Zyl, A., de Wet-Roos, D., Sanderson, R. and Klumperman, B. (2004) The role of surfactant in controlling particle size and stability in the miniemulsion polymerization of polymeric nanocapsules, *European Polymer Journal*, vol. 40, pp. 2717–2725

Velev, O., Gurkov, T., Chakarova, S., Dimitrova, B., Ivanov, I. and Borwankar, R. (1994) Experimental investigations on model emulsion systems stabilised with non-ionic surfactant blends, *Colloids and Surfaces A: Physicochemical and Engineering Aspects*, vol. 83, pp. 43-55

- Vignali, D. (2000) Multiplexed particle-based flow cytometric assays, *Journal of Immunological Methods*, vol. 243, pp. 243-255
- Warsinke, A. (2009) Point-of-care testing of proteins, *Analytical and Bioanalytical Chemistry*, vol. 393, pp. 1393–1405
- Whitesides, G. and Stroock, D. (2001 a) Flexible methods for microfluidics, *Physics Today*, vol. 54 no. 6, pp. 42.
- Whitesides, G. Ostuni, E., Takayama, S., Jiang, X. and Ingber, D. (2001b) Soft Lithography in Biology and Biochemistry, *Annual Review of Biomedical Engineering*, vol. 3, no. 1, pp. 335-373
- Whitesides, G. (2006) The origins and the future of microfluidics, *Nature*, vol.442, pp. 368-373
- Whitehouse scientific (www.whitehousescientific.com accessed 2 December 2009)
- Wu, A., Liu, A. and Hjort, K. (2007) Microfluidic continuous particle/ cell separation via electroosmotic-flow-tuned hydrodynamic spreading, *Journal of Microelectronics and Microengineering*, vol. 17, pp. 1992-1999
- Wu, W., Wang, M., Sun, Y., Huang, W., Xu, C. and Cui, Y. (2008) Dual-colour polystyrene microspheres by two-stage dispersion copolymerisation, *Materials Letters*, vol. 62, pp. 2603-2606
- Xia, Y. and Whitesides, G. (1998) "Soft lithography", *Annual Review of Materials Science*, vol. 28, no. 1, pp. 153-184
- Yasukawa, T., Suzuki, M., Sekiya, T., Shiku, H. and Matsue, T. (2007) Flow sandwich-type immunoassay in microfluidic devices based on negative dielectrophoresis, *Biosensors and Bioelectronics*, vol. 22, pp. 2730-2736

## References

---

Yates, M., Birnbaum, E. and McCleskey, T. (2000) Colored Polymer Microparticles through Carbon Dioxide-Assisted Dyeing, *Langmuir*, vol. 16, No. 11, pp. 4757-4760

Yeh, C., Hung, C., Chang, T., Lin, H. and Lin, Y. (2009) An immunoassay using antibody- gold nanoparticle conjugate, silver enhancement and flatbed scanner, *Microfluidics and Nanofluidics*, vol. 6, pp. 85-91

Yguerabide, J., Yguerabide, E., Kohne, D. and Jackson, J. (2001) [6214560](#)  
Warchol, J., Brelifiskal, R. and Herbert, D (1982) Analysis of Colloidal Gold Methods for Labelling Proteins, *Histochemistry*, vol. 76, pp. 567-575

Zhang, Y. and Lu, M. (2007) Labelling of silica microspheres with fluorescent lanthanide-doped LaF<sub>3</sub> nanocrystals. *Nanotechnology*, vol. 18: pp. 1-5

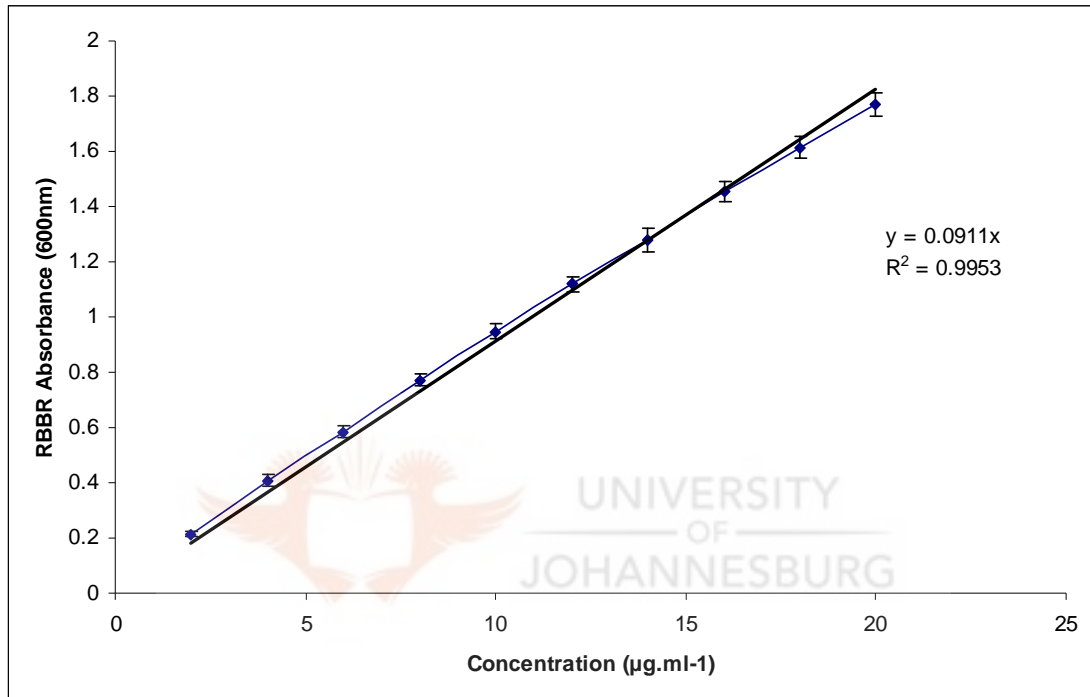




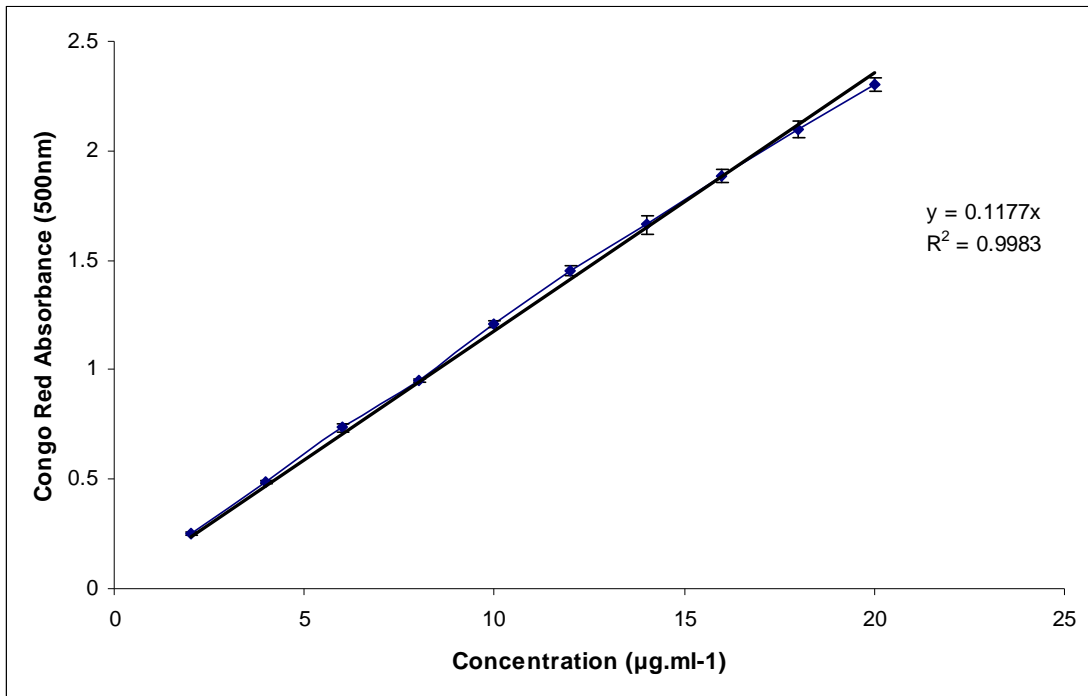
**APPENDICES**

**Appendix 1**

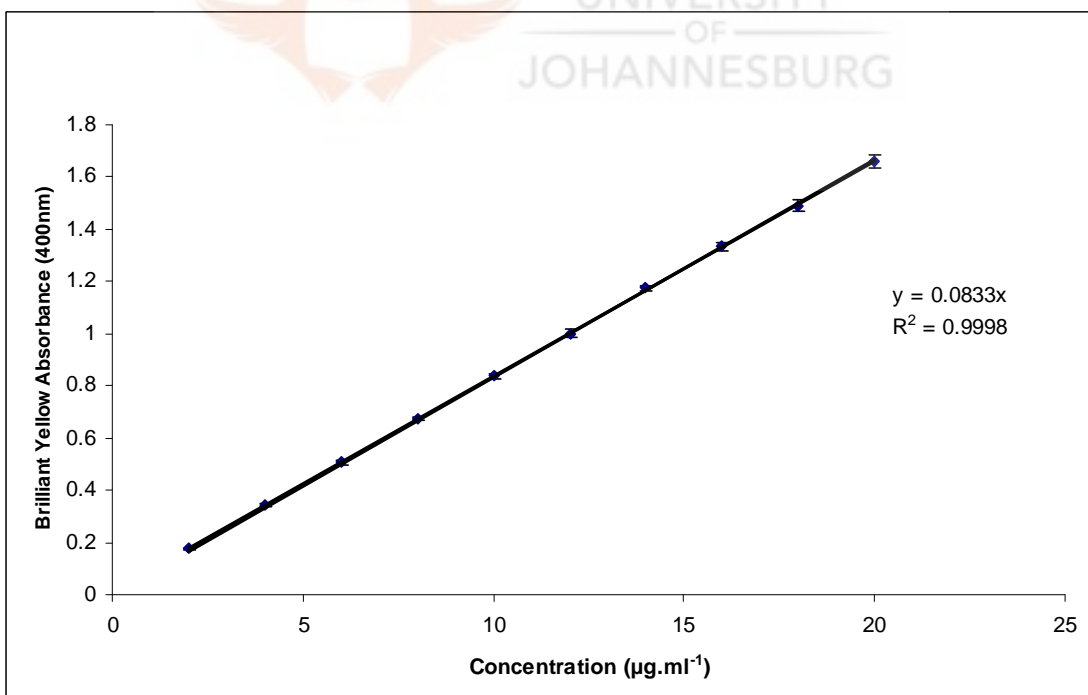
Standard curves of the different dyes used to determine the amount of dye bound to the particles



Standard curve of RBBR dye.



Standard curve of Congo Red dye.



Standard curve of Brilliant Yellow dye.

**Appendix 2**

Table summarising the different dyes screened for dye-particle interactions

| Dye                          | NaCl (ionic) | Ethanol<br>(hydrophobic) | Chloroform<br>(non polar) |
|------------------------------|--------------|--------------------------|---------------------------|
| Remazol Brilliant Blue R     | N            | N                        | N                         |
| Brilliant Yellow             | N            | N                        | N                         |
| Congo Red                    | N            | N                        | N                         |
| Remazol red (RGB)            | N            | N                        | 0                         |
| Eosin                        | Y            | Y                        | 0                         |
| Reactive Orange 14           | N            | N                        | 0                         |
| Acridine Orange              | N            | Y                        | 0                         |
| Azure II                     | N            | N                        | 0                         |
| Fuschin Magenta              | N            | Y                        | 0                         |
| Fuschin Acid                 | Y            | N                        | 0                         |
| Acid violet 9                | Y            | Y                        | 0                         |
| Methyl Green                 | N            | N                        | 0                         |
| Amide Black                  | Y            | Y                        | 0                         |
| Erronyl Black                |              |                          | 0                         |
| Levafix Brilliant Blue E-BRA | N            | Y                        | 0                         |
| Levafix Blue                 | N            | Y                        | 0                         |
| Lanaset Blue ZR              |              | Y                        | 0                         |
| Methylene Blue               | N            | N                        | 0                         |
| Brilliant Blue G             |              | Y                        | 0                         |
| Indigo Carmine               | Y            | Y                        | 0                         |

\*Leaching (Y) No leaching (N) Not tested (0)

The different dyes were screened for application in this study. Dyes that were eluted following treatment with solvents and salts were excluded. The visual properties of the dyed particles using microscopy were also used as a criterion for the selection of dyes.

**Appendix 3**

Surface area- volume calculations

Surface Area=  $4 \cdot \pi \cdot r^2$

6  $\mu\text{m}$  particles       $1.13\text{E}^{-10}$  m

13  $\mu\text{m}$  particles       $5.30\text{E}^{-10}$  m

20  $\mu\text{m}$  particles       $1.25\text{E}^{-9}$  m

Volume= $\frac{4}{3} \cdot \pi \cdot r^3$

6  $\mu\text{m}$  particles       $1.13\text{E}^{-8}$   $\mu\text{l}$

13  $\mu\text{m}$  particles       $1.15\text{E}^{-7}$   $\mu\text{l}$

20  $\mu\text{m}$  particles       $4.18\text{E}^{-7}$   $\mu\text{l}$

Number of particles = volume/ number of particles

6  $\mu\text{m}$  particles       $1.799\text{E}^{10}$   $\mu\text{l}$

13  $\mu\text{m}$  particles       $1.739\text{E}^9$   $\mu\text{l}$

20  $\mu\text{m}$  particles       $4.780\text{E}^8$   $\mu\text{l}$

**Appendix 4**

Mole dye binding

Molecular Weight

RBBR (50%)                      696.67 g.mol<sup>-1</sup>

Congo Red (85%)                625.56 g.mol<sup>-1</sup>

Brilliant Yellow (40%)        624.56 g.mol<sup>-1</sup>

$n = m/Mw$

$n = \text{mol}$

$m = \text{mass (g)}$

$Mw = \text{Molecular weight (g.mol}^{-1}\text{)}$

→ Number of moles of dye bound per particle

= mol/particle

→ Number of moles of dye bound per mass of particles

$m = \text{mass of dye bound to particles (g)}$

$Mw = \text{dye Molecular weight (g.mol}^{-1}\text{)}$